

**A STUDY OF THE PRESSURE-INDUCED
FUNDAMENTAL BAND OF DEUTERIUM IN PURE
GAS AND DEUTERIUM-FOREIGN GAS MIXTURES
AT LOW TEMPERATURES DOWN TO 77 °K**

CENTRE FOR NEWFOUNDLAND STUDIES

**TOTAL OF 10 PAGES ONLY
MAY BE XEROXED**

(Without Author's Permission)

BIDHU BHUSHAN P. SINHA

16676



A STUDY OF THE PRESSURE-INDUCED
FUNDAMENTAL BAND OF DEUTERIUM IN PURE GAS
AND DEUTERIUM-FOREIGN GAS MIXTURES AT
LOW TEMPERATURES DOWN TO 77°K

by



Bidhu Bhushan P. Sinha, M.Sc.

Submitted in partial fulfilment
of the requirements for the degree of Master of Science
Memorial University of Newfoundland

April, 1967.

This thesis has been examined and approved by:

S. P. Reddy, B.Sc.(Hons.), M.Sc., D.Sc.,

Assistant Professor of Physics,


Memorial University of Newfoundland,

and

J. L. Hunt, B.A., M.A., Ph.D.,

Associate Professor of Physics,

University of Guelph.



ABSTRACT

The pressure-induced fundamental vibration-rotation absorption band of deuterium was studied in the pure gas for gas densities up to 175 Amagat at ice, alcohol-dry ice and liquid nitrogen temperatures respectively, and in deuterium-helium and deuterium-neon mixtures for partial foreign gas densities up to 647 Amagat at 77.3°K. The shapes of the absorption contours obtained in each case were discussed. The contours of pure deuterium exhibited sharper individual branches of the fundamental band with the decreasing temperature as expected. The magnitude of the splitting of the Q branch at a constant density decreased as the temperature was lowered, disappearing at 77.3°K in the low density region while indicating a gradual re-appearance with higher density. The enhancement absorption profiles of the band in deuterium-helium and deuterium-neon mixtures showed a marked splitting of the Q branch at 77.3°K. The distinct indication of the S(0), S(1) and S(2) lines and the density-dependence of the minima of the Q branch observed in deuterium-neon mixtures was found to be absent in deuterium-helium mixtures. Binary and ternary absorption coefficients were determined for pure deuterium and deuterium-foreign gas mixtures. Applying the theory of Van Kranendonk and using the known molecular parameters of deuterium, the binary absorption coefficients of the individual lines of the O and S branches and of the quadrupole part of the Q branch were calculated and hence the overlap part was estimated. Van Kranendonk's theory was used to calculate the theoretical values of the total binary absorption

II

coefficients, $\tilde{\alpha}_1$, of pure deuterium at various temperatures in the region 300°K - 40°K, for comparison with the available experimental values obtained from various sources including the present investigation. Theoretical variation curves of $\tilde{\alpha}_1$ with temperature drawn for $\sigma/\rho = 10.00$, 11.80 and 7.94 are discussed.

TABLE OF CONTENTS

CHAPTER	Page
1 INTRODUCTION	1
1.1 The Pressure-Induced Fundamental Bands of Hydrogen and Deuterium	1
1.2 Other Infrared Absorptions of Hydrogen	4
1.3 The Origin and Theory of Pressure-Induced Infrared Absorption Spectra	5
1.4 Present Investigation	6
2 EXPERIMENTAL TECHNIQUE	9
2.1 Design and Construction of a High Pressure Low Temperature Absorption Cell	9
2.2 Optical Arrangement	14
2.3 Pure Deuterium Experiments at Ice, Alcohol-Dry Ice and Liquid Nitrogen Temperatures	16
2.4 Deuterium-Foreign Gas Mixtures at Liquid Nitrogen Temperature	19
2.5 Reduction of Experimental Traces	21
3 ISOTHERMAL CALCULATIONS	23
3.1 Isothermal Calculations for Pure D ₂ at 0°C, -72°C and -195.8°C	23
3.2 Isothermal Calculations for D ₂ -Foreign Gas Mixtures at -195.8°C	26

CHAPTER		Page
4	RESULTS AND DISCUSSION	32
4.1	Pure Deuterium Gas	32
(i)	The Absorption Contours	32
(ii)	The Absorption Coefficients	38
(iii)	Discussion	44
4.2	Deuterium Foreign Gas Mixtures at 77.3°K	48
(i)	The Absorption Profiles	48
(ii)	The Absorption Coefficients	54
(iii)	Discussion	59
5	THEORY AND CALCULATIONS	67
5.1	The Theory of the Binary Absorption Coefficients	67
(i)	Van Kranendonk's Expression for Binary Absorption Coefficients of a Pure Gas	67
(ii)	The Enhancement Binary Absorption Coefficients of Gas Mixtures	70
5.2	Calculations	71
5.3	Variation of the Binary Absorption Coefficient with Temperature	72
5.4	Conclusion	78

CHAPTER 1

INTRODUCTION

1.1 The Pressure-Induced Fundamental Bands of Hydrogen and Deuterium

The pressure-induced fundamental absorption band of hydrogen was first observed by Welsh, Crawford and Locke (1949) in compressed gaseous hydrogen. Chisholm and Welsh (1954) investigated this band in pure hydrogen and in hydrogen-foreign gas mixtures at pressures up to 1500 atmospheres at temperatures ranging from 376° to 78°K. Later, Hare and Welsh (1958) extended these studies at room temperature at pressures up to 5000 atm. Recently a detailed study of the absorption profiles of the fundamental band of hydrogen in the pure gas as well as in hydrogen-foreign gas binary mixtures at lower pressures in the temperature range 300°K to 78°K was made by Hunt and Welsh (1964). More recently the same band was studied in pure hydrogen and in hydrogen-helium mixtures at low pressures in the temperature range 18° to 77°K by Watanabe and Welsh (1964, 1965) who verified the theoretical prediction of bound states of the binary complexes $(H_2)_2$.

The induced infrared fundamental band of hydrogen was also studied quite extensively in the liquid and solid states with various ortho-para ratios by Allin, Hare and Welsh (1955), Allin and Welsh (1955) and Gush, Hare, Allin and Welsh (1960) and in hydrogen dissolved in liquid argon by Ewing and Trajman (1964). While these studies at low temperatures revealed a well-resolved rotational structure of the absorption band, additional information about the collision-induced spectra was obtained.

Deuterium, although an isotope of hydrogen, has not been studied as extensively as hydrogen. A preliminary study of the induced fundamental band of deuterium was first made by Chisholm (1952). Recently a detailed investigation of this band was made at room temperature in our laboratory by Reddy and Cho (1965a) in the pure gas and by Pai, Reddy and Cho (1966) in deuterium-foreign gas mixtures. Previously a few studies on the fundamental band of deuterium were made in the liquid and solid states by Allin, Gush, Hare, Hunt and Welsh (1959) and in gaseous phase by Watanabe and Welsh (1965) at low densities in the low temperature range from 24.0°K to 77.3°K. As for hydrogen, Watanabe and Welsh have also verified the existence of the three bound states of $(D_2)_2$ complex.

The general appearance of the pressure-induced fundamental band of deuterium differs considerably from that of hydrogen. To illustrate this, a schematic diagram of the rotational energy levels for the fundamental vibration absorption band of deuterium is presented in Fig. 1, where the possible rotational transitions in the induced fundamental band of deuterium are indicated by vertical lines with arrowhead. The approximate positions of the rotational lines, calculated from the molecular constants of the free molecule determined from the Raman spectrum of gaseous deuterium (Stoicheff 1957), are marked under the corresponding transitions. These transitions result from the selection rule $\Delta J=0, \pm 2$ giving rise to the Q, S and O branches respectively. This selection rule is the same as that for the vibrational Raman spectra of diatomic molecules. Here J is the rotational quantum number. The relative population of the molecules at room temperature in each rotational energy level, as calculated

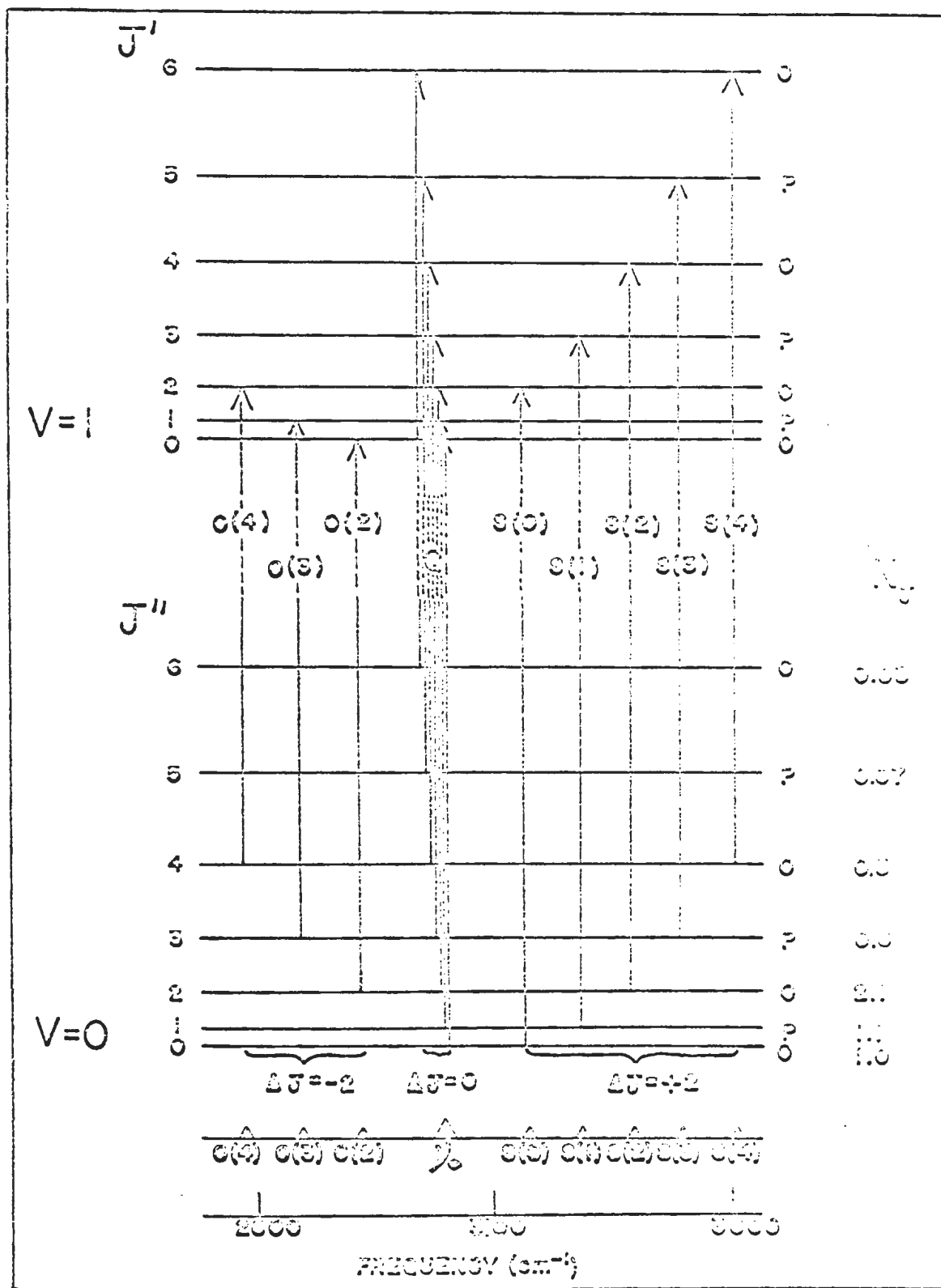


Fig. 1 Energy level diagram of the induced fundamental band of deuterium.

from the Boltzmann distribution law and the statistical weights of the level, arising from the $(2J + 1)$ - fold degeneracy and the nuclear spin ($I = 1$), is also shown in Fig. 1.

Since the rotational constant of deuterium is half that of hydrogen, the rotational levels of the lowest vibrational state of deuterium will have relatively higher population than that of hydrogen at the same temperature. Moreover the nuclear spin angular momentum of a deuterium atom is \hbar units giving a statistical weight ratio of 2:1 for states of even and odd J values respectively, for deuterium molecules, whereas this ratio is 1:3 for hydrogen molecules because the nuclear spin angular momentum for a hydrogen atom is $\hbar/2$. Thus, it is possible to expect more rotational lines in each branch of the fundamental band of deuterium than in the corresponding branch of hydrogen. In Fig. 1, each rotational energy level was indicated as O or P corresponding to ortho or para modification respectively.

1.2 Other Infrared Absorptions of Hydrogen.

The induced first overtone band of hydrogen was investigated by Welsh, Crawford, MacDonald and Chisholm (1951), and later by Hare and Welsh (1958). The pure rotational spectrum of hydrogen was observed for the first time by Ketelaar, Colpa and Hooge (1955). A more detailed study was made by Colpa and Ketelaar (1958), Kiss, Gush and Welsh (1959) and Kiss and Welsh (1959). The latter authors found that the rotational spectrum appeared to be superimposed on a continuum which was assumed to arise from translational absorption. These authors made a detailed analysis of the shape of rotational lines and found that an individual

line in the pure rotational spectrum of hydrogen at 80°K could be well represented by a dispersion line shape for the high frequency wing of the line and by a dispersion line shape modified by the Boltzmann factor for its low frequency wing. By assuming a similar shape for the lines, Hunt and Welsh (1964) made an analysis of the absorption contours of the induced fundamental band of hydrogen.

1.3 The Origin and Theory of Pressure-Induced Infrared Absorption Spectra.

Pressure-induced infrared absorption spectra of homonuclear diatomic molecules correspond to transitions, forbidden in isolated molecules, which appear when the molecules are in the form of a compressed gas, liquid or solid. The reason for the homonuclear molecules such as hydrogen, deuterium, nitrogen, oxygen, etc., to have forbidden transitions is that they do not possess a permanent electric dipole moment. Infrared absorption is observed in these molecules as a result of dipole moments induced in colliding pairs of molecules by intermolecular forces which produce a distortion of the charge configuration in the molecules. The induced dipole moment depends, in magnitude, on the intermolecular distance and the internuclear distance and, in direction, on the relative orientations of the colliding molecules. Consequently, the colliding pair of molecules gives rise to transitions in absorption at its vibrational and rotational frequencies. The intensity of the induced absorption depends on the magnitude of the induced dipole moment which in turn depends on several molecular parameters of the colliding pairs.

The theory of the induced fundamental band of homonuclear diatomic molecules has been given by Van Kranendonk and Bird (1951), Van Kranendonk, (1952, 1957, 1958) and Britton and Crawford (1958) who have shown that the absorption due to binary collisions must be explained in terms of electron overlap interaction and molecular quadrupole interaction. Based on the assumption of an "exp-4" model, the electric dipole moment, induced by the short-range overlap forces, decreases exponentially with the inter-molecular distance R and is, in the first-order approximation, spherically symmetric, i.e., almost independent of the relative orientations of the molecules in a colliding pair. This produces mainly transitions for which $\Delta J = 0$ (Q-branch). On the other hand the electric dipole moment, induced by long-range quadrupole interaction, varies as R^{-4} and is strongly dependent on the mutual orientation of the colliding pair and produces transitions for which $\Delta J = \pm 2$ (S and O branches) and in addition, some contribution to the intensity of the Q-branch.

The above theory has been frequently applied to the experimental results obtained in the studies of pressure-induced fundamental bands of homonuclear diatomic molecules. While the theory was found satisfactory in the higher temperature region, the disagreement between the theoretical and experimental values of the binary absorption coefficients becomes pronounced in the low temperature region below 80°K for both hydrogen and deuterium.

1.4 Present Investigation.

In the present investigation, a detailed study of the fundamental band of deuterium was made in the pure gas at ice point (273.1°K), ethyl

alcohol-dry ice mixture temperature (201.2°K), and liquid nitrogen temperature (77.3°K) up to a maximum density of 175 Amgt. The study of the same band was extended, at liquid nitrogen temperature, to deuterium-helium mixtures at densities up to 650 Amgt and to deuterium-neon mixtures up to 390 Amgt. Several interesting features of the absorption profiles obtained in each case were qualitatively discussed. Binary and ternary absorption coefficients were determined for the fundamental band of deuterium in pure deuterium and in deuterium-helium and deuterium-neon mixtures at the temperatures studied.

Prior to the present work, the binary absorption coefficients of the fundamental band of deuterium in the pure gas were determined by Reddy and Cho (1965) and Chisholm (1952) at 300°K and by Watanabe and Welsh (1965) in the temperature range from 20°K to 80°K . The present study now supplies their values at the three temperatures mentioned above. The fundamental band of deuterium was studied in deuterium-neon mixtures for the first time.

Applying the theory of Van Kranendonk (1958) and using the known molecular constants of deuterium, helium and neon, the binary absorption coefficients of the individual lines of the O and S branches and of the quadrupole part of the Q branch of the band were calculated in each case. The overlap parts of the binary absorption coefficients of the Q branch were estimated by subtracting the calculated quadrupole binary absorption coefficients from the experimental values of the corresponding total binary absorption coefficients.

Finally, an attempt was made to compare the variation with temperature of the observed binary absorption coefficient of the deuterium fundamental band in the pure gas with the corresponding theoretical variation as predicted by the theory of Van Kranendonk.

CHAPTER 2

EXPERIMENTAL TECHNIQUE

2.1 Design and Construction of a High Pressure Low Temperature Absorption Cell.

The transmission-type absorption cell shown in Fig. 2 was specially designed by the author for the present investigation. It was made of a stainless steel (Type No. 303) cylinder, A, 15.5 in. long and 3.2 in. in diameter, with a central bore of $3/4$ in. A stainless steel light guide, G, made in two sections, with a central rectangular cross section $3/8$ in. x $3/16$ in. was inserted into the central bore. The inside surface of the light guide was polished to ensure a good reflection of radiation. The entrance and exit windows, W, were optically flat synthetic sapphire plates, 1 in. in diameter and 5 mm. thick. They were cemented on to the stainless steel window plates, P, with a thin layer of General Electric Silicone rubber cement.

The surfaces of the window plates, were also optically flat to ensure a very good pressure seal. The windows were secured by steel caps, C, with teflon washers occupying the rest of the spaces inside the caps. The window plates had rectangular apertures, $3/8$ in. x $3/16$ in. The apertures of the cell were designed to allow a $f/4$ cone of radiation to focus the source and spectrometer slit on the entrance and exit ends of the cell respectively. After several trials, a successful design for the seats, SPD, for the invar rings, R, $1/8$ in. thick, between the window plates, P, and the body of the cell, was obtained. The details of the design of the seats SPD are shown separately in Fig. 3. The invar rings,

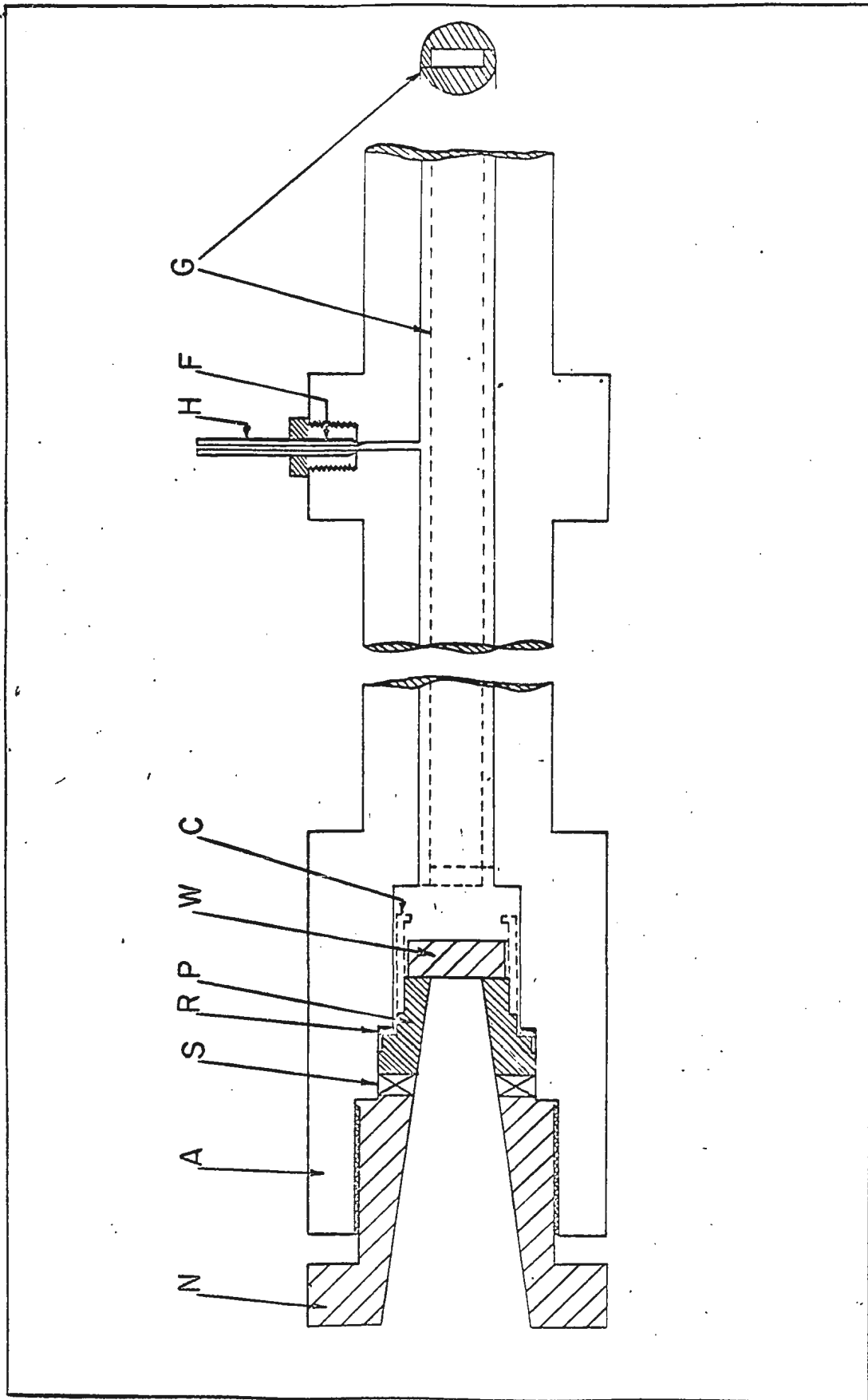


Fig2. Design of a gas absorption cell for high pressure and low temperature

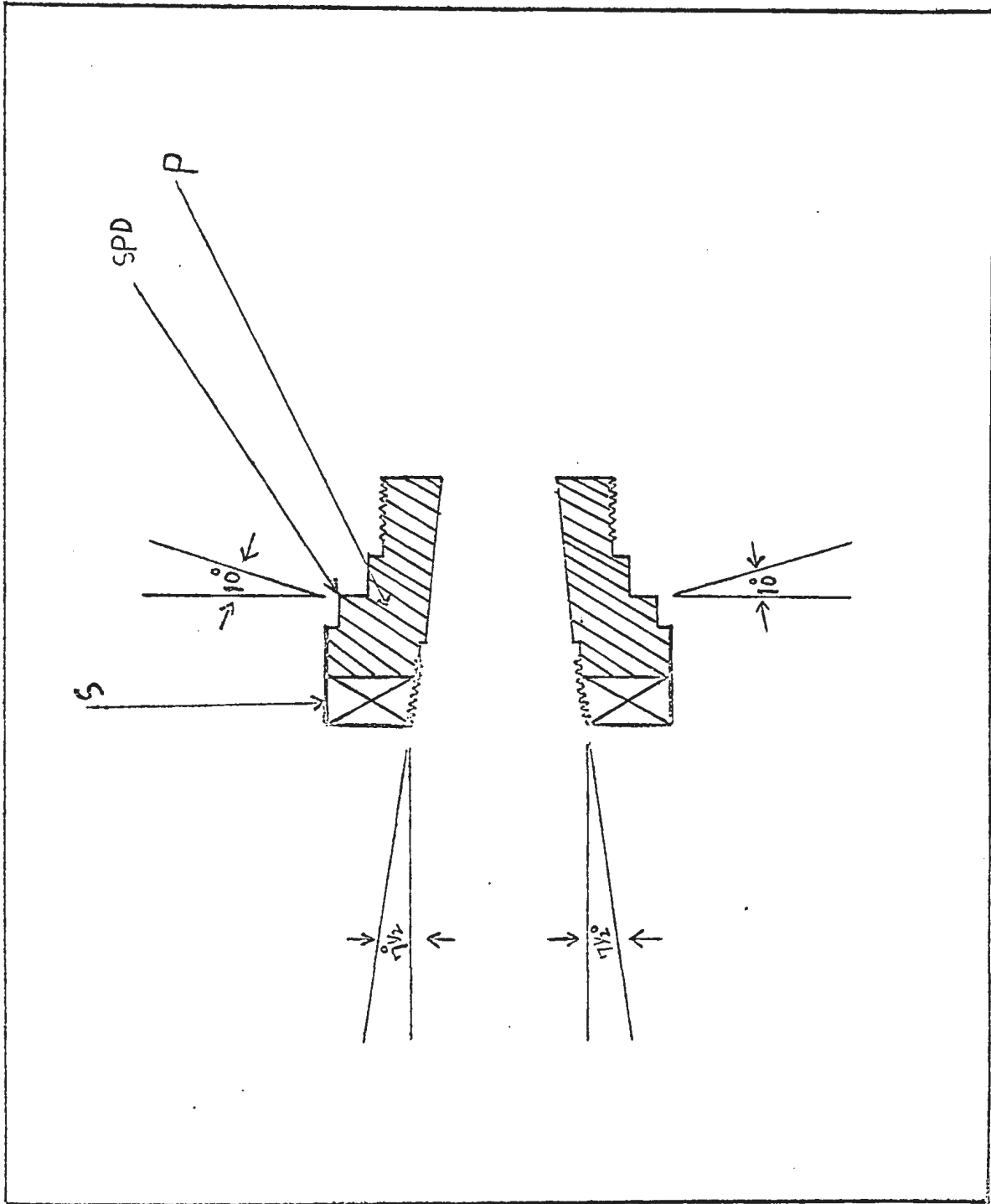


Fig. 3. Design of the Seat for Pressure Seal.

R, (Fig. 2) were made to fit exactly into these seats. This design maintained the pressure seal even at liquid nitrogen temperature. The portion, S, of the window plates with a thickness of 0.35 in. was square in shape and fitted into a matched square recess in the cell body, so as to prevent the non-alignment of the light guide and the apertures of the window plates when the hexagonal stainless steel closing nuts, N, (Fig. 2) were tightened to hold the cell "pressure-tight". A 1/4 in. diameter steel capillary tube, H, (Fig. 2) served as the gas inlet to the cell and was connected by means of an Aminco-fitting, F. The cell was tested for pressures up to 1200 atm at room temperature and up to 400 atm at liquid nitrogen temperature.

The design of this high pressure low temperature absorption cell differs to some extent from that of Kiss, Gush and Welsh (1959).

The outer system of the gas absorption cell consisting of outer jacket and end pieces is shown schematically in Fig. 4. The cell body was surrounded by an outer jacket, J (Fig. 4), to hold the coolant for low temperature experiments. This jacket, J, consisted of a thin galvanized iron sheet detachable into two separate parts which are supported at the ends by brass pieces, B (Fig. 4), and was held tight to the cell body by means of rubber "O" rings and steel nuts, T (Fig. 4). It was insulated by means of styrofoam, I (Fig. 4).

The condensing system used in the end pieces of the cell served to protect the inner windows of the cell against fogging at low temperatures. A steel extension tube, E, cemented into the hexagonal nut, N, by a thin

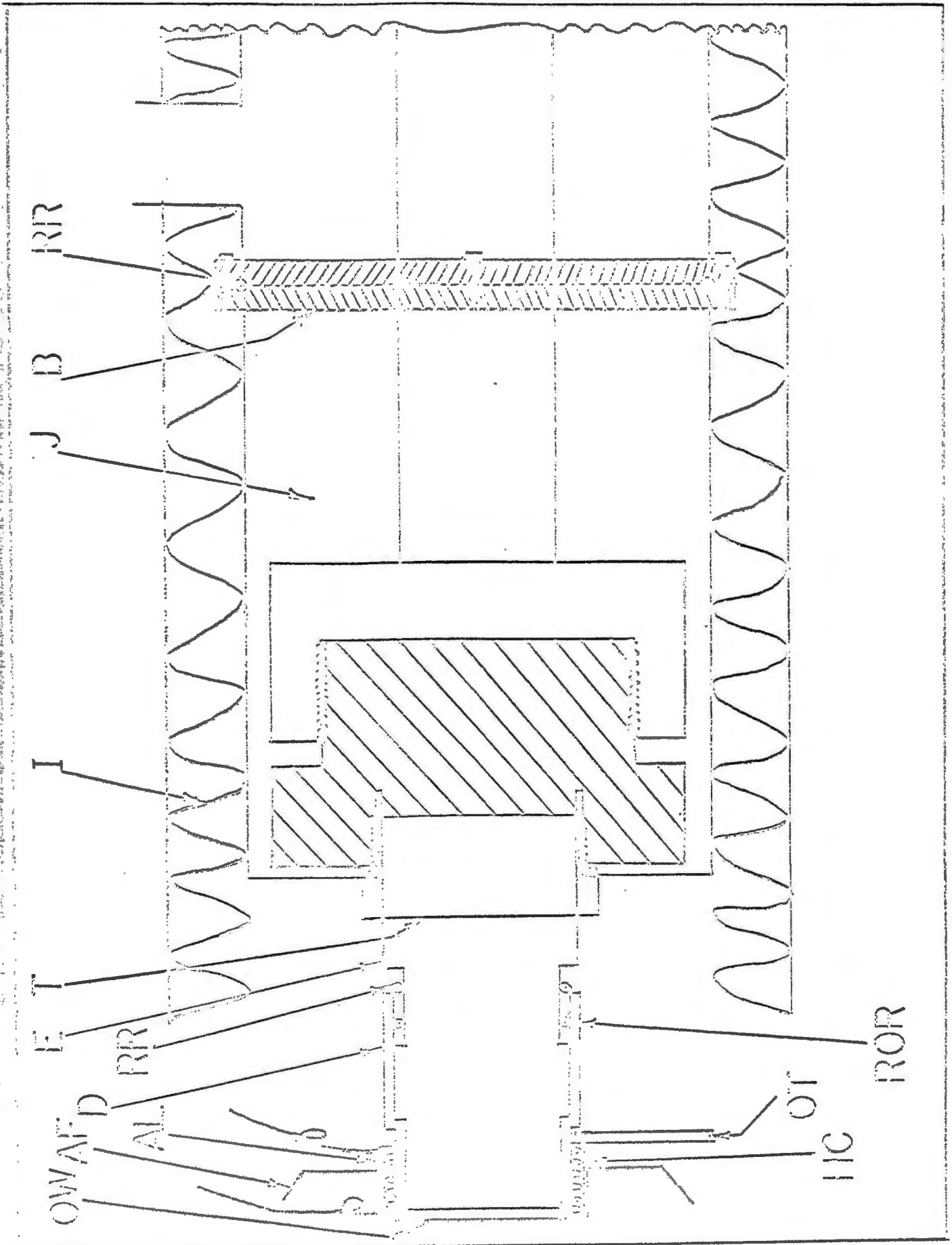


Fig.4. Outer jacket and end-pieces of the absorption cell

layer of General Electric Silicone rubber cement, had a groove in its outer surface to fit a rubber O ring, ROR (Fig. 4). A plastic extension tube, D, with incorporated heating coils, HC (Fig. 4) at the end side close to the outer window, OW, was pushed in over a rubber ring, ROR, to hold it air-tight. Another rubber ring, RR, which was used to close the opening of the plastic tube, D, ensured air-tightness against the walls of the two tubes, D and E. An outlet, OT, was used to evacuate the condensing system. The outer windows, OW, were optically flat synthetic sapphire plates, 1 in. in diameter and 2 mm thick, and were cemented on to the plastic tube, D, with General Electric Glyptal cement. An electric current varying from 0.2 amp. to 0.7 amp. was maintained in the heating coils, HC, to prevent fogging at the outer window, OW, at different stages of the low temperatures. For liquid nitrogen temperature experiments, aluminium foils, AF, of concave shutter type were used to protect the outer windows against the rushing cold draft of nitrogen vapours.

The optical path length of the absorption cell was noted after taking into consideration the contraction of the cell body at low temperature. It was 25.8 cm at the ice point and 25.7 cm at both dry ice-alcohol temperature and at liquid nitrogen temperature. The figures are correct up to one decimal place only.

2.2 Optical Arrangement.

The optical arrangement used with the transmission cell is shown in Fig. 5. Infrared radiation from the source, S, was focussed through the outer window on the entrance window of the cell, H, by means of a spherical mirror, M1, whose front surface is aluminized. The radiation

*Pai, S. T., 1965, M.Sc. Thesis, Memorial University of Newfoundland.

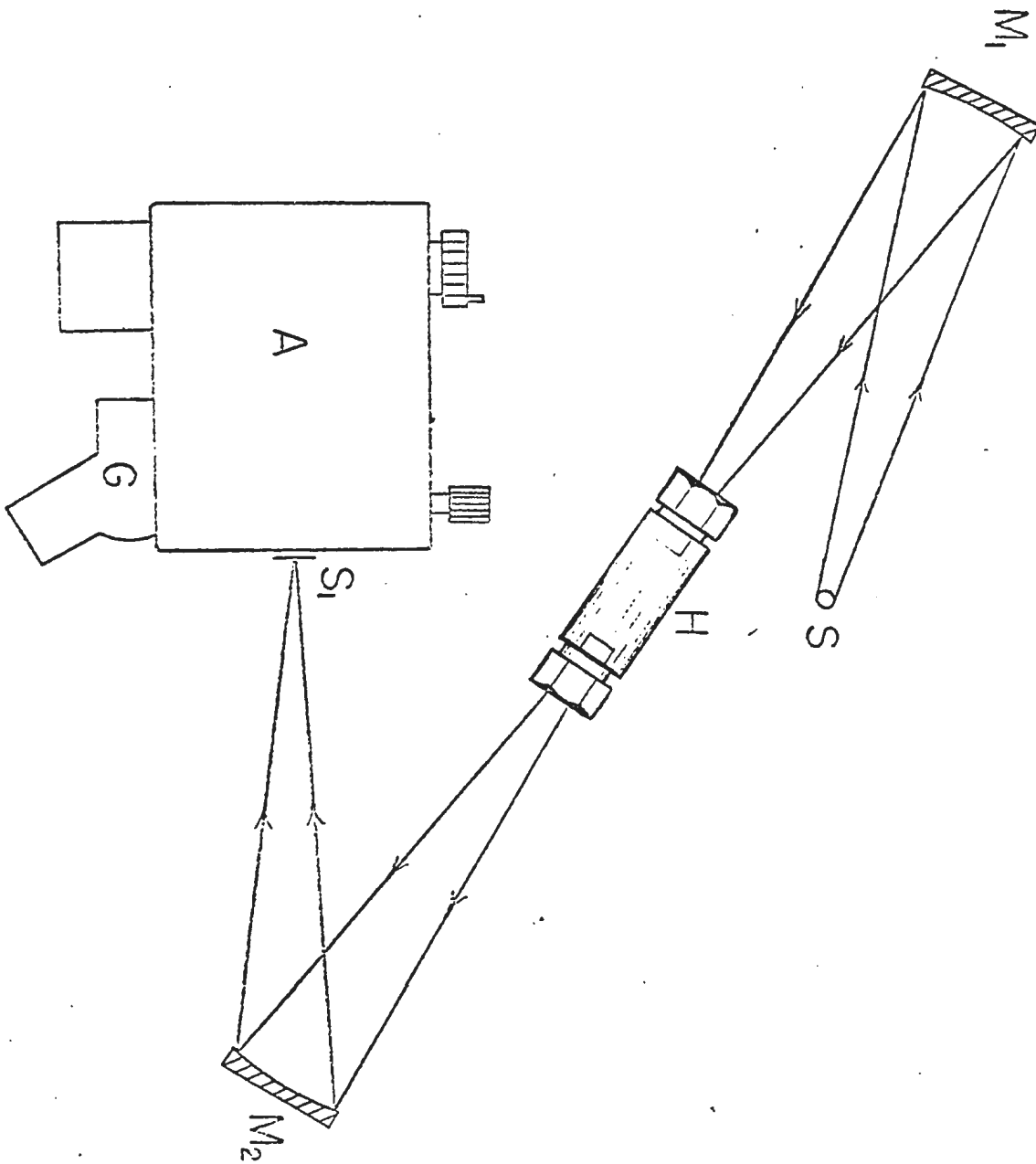


Fig. 5. The optical arrangement.

emerging through the second outer window from the exit window of the cell was focussed on the slit, S1, of the spectrometer, A, by a second aluminized spherical mirror, M1. To match the internal optics of the spectrometer, a f/4 light cone was used throughout the external arrangement.

A Perkin-Elmer 12C Spectrometer with LiF prism and a Unicam Pneumatic Golay Detector, G, were used to record the spectra. A water-cooled globar operated at 150 watts from a Sorenson voltage regulator was used as the source of the infrared continuum. The spectrometer slit width was maintained at 200μ which gave a spectral resolution of approximately 11 cm^{-1} at 2992 cm^{-1} the origin of the fundamental vibrational band of deuterium. The spectral region from $2,400\text{ cm}^{-1}$ - $4,000\text{ cm}^{-1}$ was calibrated using water bands and liquid indene bands of known frequencies (Thomson, I.U.P.A.C. 1961).

2.3 Pure Deuterium Experiments at Ice, Alcohol-Dry Ice and Liquid Nitrogen Temperatures.

A high pressure gas system, shown schematically in Fig. 6, comprised of a mercury-column gas compressor, pressure gauges, needle valves, etc., was used for the introduction of gases in the absorption cell.

Prior to each experiment with pure deuterium gas at three different low temperatures, namely ice fixed point, ethyl alcohol dry ice temperature and liquid nitrogen temperature, the following initial steps were taken, in order:

- 1) The entire system was evacuated to a pressure of 0.1 mm of Hg for several hours.

*Pai, S.T., 1965, M.Sc. Thesis, Memorial University of Newfoundland.

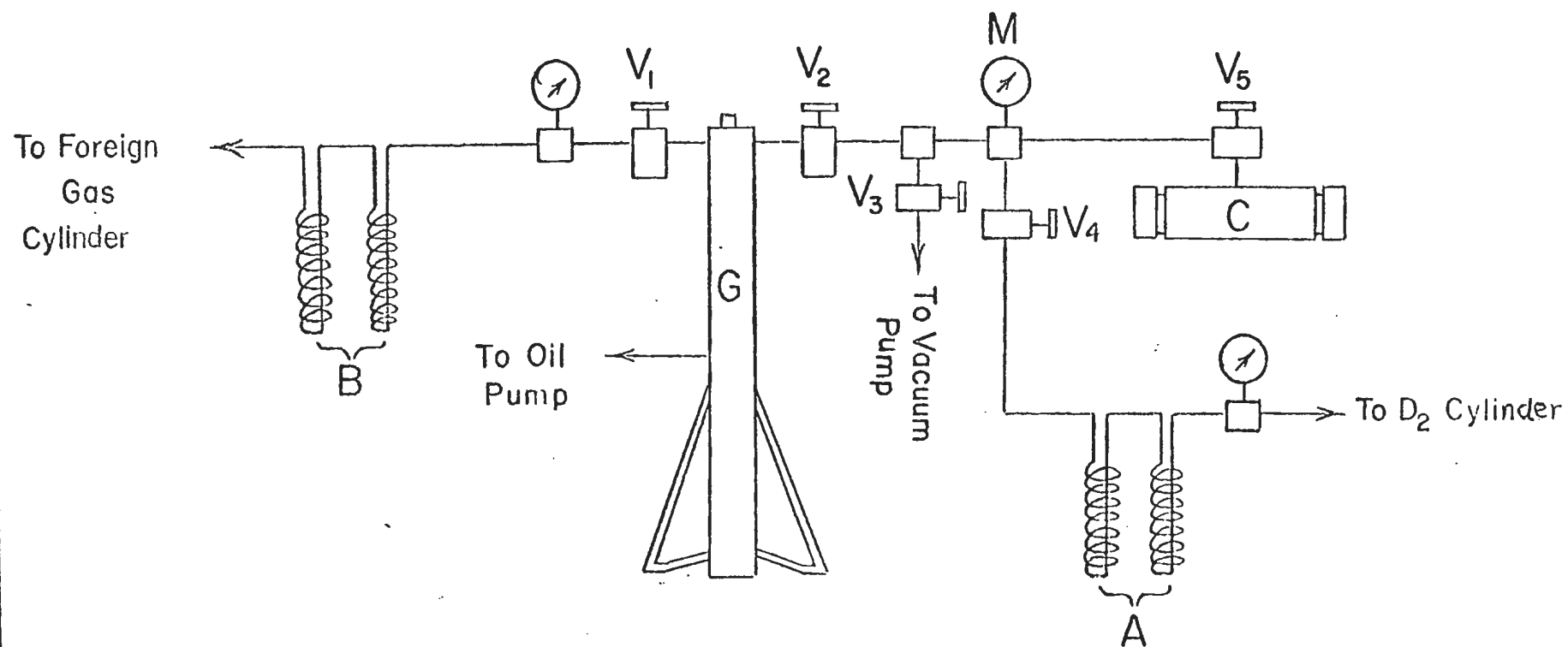


Fig. 6. The high pressure gas system.

- 2) The absorption tube was cooled down to the desired temperature by means of a suitable coolant and current was passed in the heating coils to prevent fogging on the outer windows.
- 3) The background spectrum was recorded repeatedly until a good reproduction was obtained.

In each experiment deuterium gas from a commercial cylinder, supplied by Matheson Company of Canada, at an initial pressure of 1400 psi, was admitted into the absorption cell through a system of two liquid-nitrogen traps A, and needle valves V_4 and V_5 . Prior to this, the valve V_2 was closed to isolate the gas compressor G, which was found unnecessary for pure deuterium experiments. After admitting deuterium into the absorption cell at the required pressure as read by both Bourdon-type gauges M and M_1 , the valve V_4 was closed.

The ice temperature was obtained and maintained by precooling the absorption cell by liquid nitrogen and keeping the cell covered with powdered ice in the outer jacket. A thermometer dipped in the ice touching the body of the cell read the temperature of the cell.

The alcohol-dry ice temperature was obtained and maintained by precooling the cell and filling in the outer jacket with alcohol-solid carbon dioxide mixture coolant. Dry ice was added frequently after brief intervals. A low temperature thermometer made by Fisher & Co. was dipped in the coolant to ensure the consistency of the temperature.

The liquid-nitrogen temperature was obtained and maintained by filling in the outer jacket with liquid nitrogen to keep the absorption cell always dipped in the coolant.

The ice fixed point is taken as 273.16°K (0°C), alcohol-dry ice temperature as 201.16°K (-72°C) and liquid nitrogen temperature as 77.3°K (-195.8°C) from the tables given in the Handbook of Chemistry and Physics (1960) by the Chemical Rubber Publishing Co.

The pressure gauge, M, was calibrated against a dead-weight pressure balance up to a maximum of 20,000 psi, while, M_1 , called Master gauge was calibrated up to 3,000 psi.

2.4 Deuterium-Foreign Gas Mixture Experiments at Liquid Nitrogen Temperature.

Here the initial steps were similar to those described above. The gases used in this investigation were introduced into the absorption cell by the high pressure gas system shown in Fig. 6. In each experiment, deuterium gas at a given base pressure was first admitted into the cell, C, from a commercial cylinder, supplied by Matheson Co. of Canada Ltd., through two liquid nitrogen traps, A, and needle valves, V_4 and V_5 , after closing the valve, V_2 . Valves, V_4 and V_5 were then closed. Absorption spectrum of the pure D_2 gas was then recorded until a good reproduction of the traces was obtained. Then the part between the needle valves, V_2 , V_5 , and V_4 , was re-evacuated. Traces for the absorption of deuterium gas in the cell were taken again to ensure the perfect functioning of the controlling valve, V_5 . The component foreign gas was then introduced

into the gas compressor, G, through two liquid nitrogen traps, B. The gas compressor was of mercury column type and the compression was achieved by means of a column of mercury driven by a hand-operated Aminco oil pump in conjunction with a pressure intensifier (although the intensifier part was not used in the present investigations to achieve the desired pressure range). The first dose of the foreign gas was admitted into the absorption cell, containing pure deuterium gas at a fixed base density by the so-called "pulsating technique". This consisted of opening the needle valve, V_5 , momentarily three or four times at proper intervals, so that the foreign gas attained the temperature of the cell which was ensured by observing no indication of any drop in pressure as read by the pressure gauge, M. The length of the steel capillary tubing connecting the valve, V_5 and the cell was made very short so that the probable experimental error caused by the imperfect mixing of gases inside the capillary tubing would become negligible. This method of "short pulses" employed in the introduction of foreign gases prevented the possible back diffusion of deuterium gas from the cell to a great extent. Previous workers in this field also used this method extensively.

It was observed that the introduction of a foreign gas into the cell caused the signal to fall off suddenly and then return gradually to the original level. This duration was 15 to 20 minutes in case of D_2 -He mixtures and 20 to 30 minutes for D_2 -Ne mixtures. It was found that the time of recovery could be shortened a little if the signal was shut off before introducing the foreign gas. Several trial traces were taken until a good reproduction was obtained, and this ensured a thorough

mixing of the gases. This procedure was repeated for different deuterium-foreign gas mixtures with fixed base densities of pure deuterium. Two different base densities of deuterium (59.7 Amgt and 46.62 Amgt) were used for D₂-He mixtures and two (61.0 Amgt and 53.2 Amgt) for D₂-Ne mixture experiments at liquid nitrogen temperature.

2.5 Reduction of Experimental Traces.

In reducing the traces of the absorption contours, the water band at 3700 cm⁻¹, which appeared in each trace, was used as a frequency reference.

In pure deuterium experiments, the contours were reduced over the background spectrum in vacuum. If I_0 is the signal transmitted by the evacuated cell of optical path length, ℓ , and I is the signal with pure deuterium gas in the cell, the reduction process by the standard logarithmic scale gave $\log_{10}(I_0/I)$, which was determined at intervals of 10 cm⁻¹ across the entire fundamental band. The absorption coefficient, $\alpha(\nu)$, is given by $(1/\ell) \log_e (I_0/I)$. The profiles of the band at different gas densities at each temperature were obtained by plotting $\log_{10} (I_0/I)$ vs ν (frequency in cm⁻¹).

In the deuterium-foreign gas mixture experiments it was required to study the enhancement in absorption when a particular gas was added to deuterium which was at a fixed base pressure in the absorption cell. In mixture experiments, if I_1 is the signal transmitted by the absorption cell of length ℓ , filled with a base density of deuterium, and I_2 is the

signal with the binary gas mixture in the cell, the enhancement in the absorption coefficient, $\alpha_{\text{enh}}(\nu)$ at a given frequency ν in cm^{-1} , is given by $(1/\ell) \log_e (I_1/I_2)$. The profiles of the enhancement absorption were obtained by plotting $\log_{10} (I_1/I_2)$ vs ν (frequency in cm^{-1}) at intervals of 10 cm^{-1} across the band.

Unlike hydrogen, ortho-deuterium molecules exist in even rotational levels ($J = 0, 2, 4, \dots$) and para molecules in odd levels ($J = 1, 3, 5, \dots$) and the ratio of para- and ortho-deuterium concentrations is 1:2 in normal deuterium. In experiments at liquid nitrogen temperature, one should consider the possibility of para-ortho conversion of normal deuterium contained in a steel absorption cell. While no special precaution was taken in the present investigation to prevent such conversion, it was found that no appreciable conversion had taken place within the period of any particular experiment. This conclusion was arrived at in the following way: In the low temperature experiments with pure deuterium, the trace obtained at a particular pressure of the gas, while the pressure was increased in steps, was compared with the one obtained at the same pressure after 4 or 5 hours, while the pressure was decreased in steps, and it was found that the two traces matched reasonably well with each other.

CHAPTER 3

ISOTHERMAL CALCULATIONS

The number of molecules of a given gas is more directly related to its density than to its pressure. It is therefore convenient to study the absorption of molecules as a function of density. In the study of the induced infrared absorption spectra of molecules, density is usually expressed in Amagat units. An Amagat unit is defined as the ratio of the density of a gas at a given pressure and temperature to its density at normal temperature and pressure (i.e. at N.T.P.). In this Chapter a brief account of the calculation of densities of deuterium, helium and neon at the experimental conditions of the present investigation is given.

3.1 Isothermal Calculations for Pure Deuterium at 0°C, -72°C and -195.8°C.

The density of pure deuterium gas at ice temperature (0°C) was directly determined from the isothermal data of Michels and Goudekot (1941). The maximum density used for ice temperature experiments was 150.5 Amagat.

The density of pure deuterium gas at alcohol - dry ice temperature (-72°C) was calculated from the available isothermal data of Michels et al (1959) for deuterium at -50°C and -75°C by the method of linear interpolation between these two points. The calculated isothermal data for pure deuterium gas at -72°C are summarized in Table I(a).

The density of pure deuterium at liquid nitrogen temperature (-195.8°C) was derived up to 49 atmospheres directly from the data available for hydrogen in NBS Technical Note 120 by Dean (1961) using the procedure outlined on page 434 of NBS RP 1932 by Woolley, Scott and Brickwedde (1948).

The compressibility factor, Z_H , for hydrogen gas is given by

$$Z_H = PV/RT = (1 + BP + CP^2 + \dots),$$

where B, C,....are the second, third virial coefficients and other terms are the same as in the usual notation. The compressibility factors for hydrogen at -195.8°C were calculated by linear interpolation method, up to 164 atmospheres from the compiled data of Woolley et al (1948). Since the deuterium isotherms run parallel to those of hydrogen, the difference between the second virial coefficient of hydrogen, B_H , and that of deuterium, B_D , (i.e. $B_H - B_D$) was calculated at liquid nitrogen temperature. The compressibility factor, Z_D , for deuterium was then calculated by subtracting $(B_H - B_D)$ from the corresponding Z_H at a series of pressures. The third virial coefficient C was neglected in calculating the compressibility factor Z_D from Z_H . In adopting this procedure, the following assumption was made and found justified. The second virial coefficient of hydrogen and deuterium at 0°C being $13.235 \text{ cm}^3/\text{mole}$ and $13.864 \text{ cm}^3/\text{mole}$ respectively, the ratio of the specific volume of hydrogen at N.T.P. to that of deuterium at N.T.P. is found to be equal to $(1 + 0.0006185)/(1 + 0.0005904) = 1.0000281$, which may be assumed to be equal to 1, as the error involved will be only a few in 10^5 . This justifies the assumption that the specific volumes of hydrogen and deuterium are almost the same within an accuracy of 0.001 % to 0.0001%.

Let the actual density of hydrogen in Amgt units be H_{2p} , while that of deuterium is D_{2p} . If the corresponding approximate densities in Amgt units as calculated from the ideal gas equation are H^0_{2p} and

TABLE I(a)

Isothermal data for deuterium at alcohol - dry ice temperature (-72°C)

P (Atmosphere)	ρ (Amagat)	P (Atmosphere)	ρ (Amagat)
10.0	13.26	120	150.11
20.0	26.34	130	161.45
30.0	39.89	140	172.56
40.0	53.02	150	183.35
50.0	65.62	160	193.65
60.0	78.40	-	-
70.0	90.72	-	-
80.0	102.98	-	-
90.0	115.11	-	-
100.0	126.84	-	-
110.0	138.66	-	-

$D_{2\rho}^0$ respectively, then $H_{2\rho}^0 = D_{2\rho}^0$. Now, $H_{2\rho} = H_{2\rho}^0/Z_H$ and $D_{2\rho} = D_{2\rho}^0/Z_D$, so that

$$(1) \quad D_{2\rho} = H_{2\rho} \times (Z_H/Z_D).$$

Thus, from a knowledge of Z_D , Z_H and $H_{2\rho}$, which are accurate enough for this purpose, the isothermal data of deuterium at liquid nitrogen temperature were calculated and summarized in Table I(b)

3.2 Isothermal Calculations for D_2 -Foreign Gas Mixtures at -195.8°C .

The isotherms of deuterium gas at liquid nitrogen temperature for higher pressures up to 165 Atm were determined by a method similar to that described above from the available data for hydrogen given by Woolley, Scott and Brickwedde (1948). Beyond 165 Atm, the isotherms were calculated from the best polynomial fit of the equation of state,

$$(2) \quad PV = RT (1 + BP + CP^2)$$

in the high pressure regions of the available data. The most suitable values of B and C were found to be as $B = -817 \times 10^{-6} (\text{Atm})^{-1}$ and $C = +110 \times 10^{-7} (\text{Atm})^{-2}$. The calculated isotherms are summarized in Table I(b).

The P - ρ relations of helium at liquid nitrogen temperature were directly derived from the data of NBS Technical Note 154 by Mann (1962) up to 110 Atm. Beyond 100 Atm the isotherms for helium were calculated again by the best polynomial fit of the equation of state (2) as explained above. The most suitable values for B and C for helium gas were found to be as $B = +1.803 \times 10^{-3} (\text{Atm})^{-1}$, and $C = +0.5167 \times 10^{-6} (\text{Atm})^{-2}$.

TABLE I(b)

Isothermal data for deuterium at liquid nitrogen temperature

P (Atmosphere)	ρ (Amagat)	P (Atmosphere)	ρ (Amagat)	P (Atmosphere)	ρ (Amagat)
0.28	1.00	59.76	218.73	164.43	500.06
0.57	2.00	65.43	240.03	180.6	525.86
0.85	3.00	71.25	260.26	200.0	553.50
1.69	6.00	77.24	279.86	220.0	574.62
2.82	10.00	83.42	300.06	240.0	589.85
5.61	20.01	89.85	320.06	260.0	599.92
11.13	40.01	96.54	340.06	280.0	605.55
16.58	60.02	103.55	360.05	300.0	607.43
21.97	80.02	110.89	380.05	320.0	606.21
27.37	100.09	118.59	400.05	340.0	602.47
32.66	120.02	126.71	420.05	-	-
37.99	139.96	135.33	440.05	-	-
43.34	159.96	144.45	460.05	-	-
48.79	180.15	154.13	480.06	-	-
54.20	200.03	160.0	491.17	-	-

The calculated isotherms of helium gas at liquid nitrogen temperature are summarized in Table II.

As a result of cross-checking with the extensive data available for helium gas at room temperature and 0°C, it was found that the method of best polynomial fit of the equation of state (2) was accurate up to 400 Atm with a probable error of 1 to 1.5%.

The P-ρ relations for neon gas at liquid nitrogen temperature were directly derived by the linear interpolation method between two close points from the available data of Timmerhaus (1963). The derived isothermal data of neon are given in Table III.

To determine the partial density of a foreign gas, ρ_b , the following interpolation method was used: (i) Assuming that the pressures of the component gases in a mixture were approximately additive, the approximate partial pressure of the foreign gas was obtained by subtracting the partial pressure of D₂ gas from the total pressure of the mixture. (ii) The approximate partial density of ^{the} foreign gas, ρ_b , was then obtained from the isothermal data given in the Table, I(b) for deuterium, and Tables II and III for helium and neon respectively. (iii) The approximate mixture ratio $\beta^{(1)} = \rho'_b / \rho_a$ was calculated next. (iv) After that, using the interpolation relation

$$(3) \quad \rho_{a+b}^{(1)} = (1/1 + \beta^{(1)}) [(\rho_a)_P + \beta^{(1)} (\rho_b)_P],$$

the mixture density, $\rho_{a+b}^{(1)}$, correct to the first approximation was determined. Here, $(\rho_a)_P$ and $(\rho_b)_P$ are the densities of deuterium and

TABLE II

Isothermal data for helium at liquid nitrogen temperature (-195.8°C)

P (Atmosphere)	ρ (Amagat)	P (Atmosphere)	ρ (Amagat)	P (Atmosphere)	ρ (Amagat)
1.0	3.53	100.0	298.07	280.0	690.24
5.0	17.52	110.0	322.67	300.0	667.79
10.0	34.75	120.0	346.48	320.0	693.75
20.0	68.31	130.0	369.52	340.0	718.22
30.0	100.69	140.0	391.82	-	-
40.0	131.96	160.0	434.33	-	-
50.0	164.08	180.0	474.20	-	-
60.0	191.18	200.0	511.64	-	-
70.0	219.24	220.0	596.81	-	-
80.0	246.44	240.0	579.87	-	-
90.0	272.64	260.0	610.97	-	-

TABLE III

Isothermal data for neon at liquid nitrogen temperature

P (Atmosphere)	ρ (Amagat)	P (Atmosphere)	ρ (Amagat)
1.0	3.56	100.0	396.06
10.0	36.18	110.0	433.72
20.0	73.72	120.0	469.69
30.0	112.51	130.0	503.82
40.0	152.40	-	-
50.0	193.13	-	-
60.0	234.35	-	-
70.0	275.68	-	-
80.0	316.69	-	-
90.0	356.94	-	-

foreign gas respectively at the total pressure of the mixture, P , which may be obtained from the isothermal data given in the Tables. (v) Then, using the relation,

$$(4) \quad \rho_b^{(1)} = \rho_{a+b}^{(1)} - \rho_a^{(1)},$$

the partial density of the foreign gas correct to the first approximation was determined. (vi) Finally, using the ratio $\beta^{(2)} = \rho_b^{(1)} / \rho_a^{(1)}$, and the interpolation relation correct to the second approximation,

$$(5) \quad \rho_{a+b}^{(2)} = (1/1 + \beta^{(2)}) [(\rho_a)_P + \beta^{(2)} (\rho_b)_P],$$

the partial density of the foreign gas, $\rho_b^{(2)}$, correct to the second approximation was found. It was usually found that the difference between the densities $\rho_b^{(1)}$ and $\rho_b^{(2)}$ was always within the probable experimental error ($\sim 2\%$). Hence, for the present investigation the density $\rho_b^{(1)}$ was accurate enough within the limits of experimental error. This method of calculating the partial densities of foreign gases is very similar to the one used by Cho et al (1963), and Reddy and Cho (1965b).

CHAPTER 4

RESULTS AND DISCUSSION

4.1 Pure Deuterium Gas.

(i) The Absorption Contours:

Figs. 7, 8, and 9 represent the observed absorption profiles of the induced fundamental band of pure deuterium at ice-point, alcohol - dry ice temperature and liquid nitrogen temperature respectively at a series of densities. The positions of the band origin, ν_0 , and the lines S(0), S(1), S(2), S(3), S(4), O(2), and O(3) were calculated from the molecular constants of the free deuterium molecules obtained by Stoicheff (1957) from the high resolution Raman spectra of gaseous deuterium and were marked on the frequency axis. Table IV(a) below summarizes the experimental conditions for which the absorption contours of the fundamental band of deuterium were obtained in the pure gas.

TABLE IV(a)

Outline of the Experiments

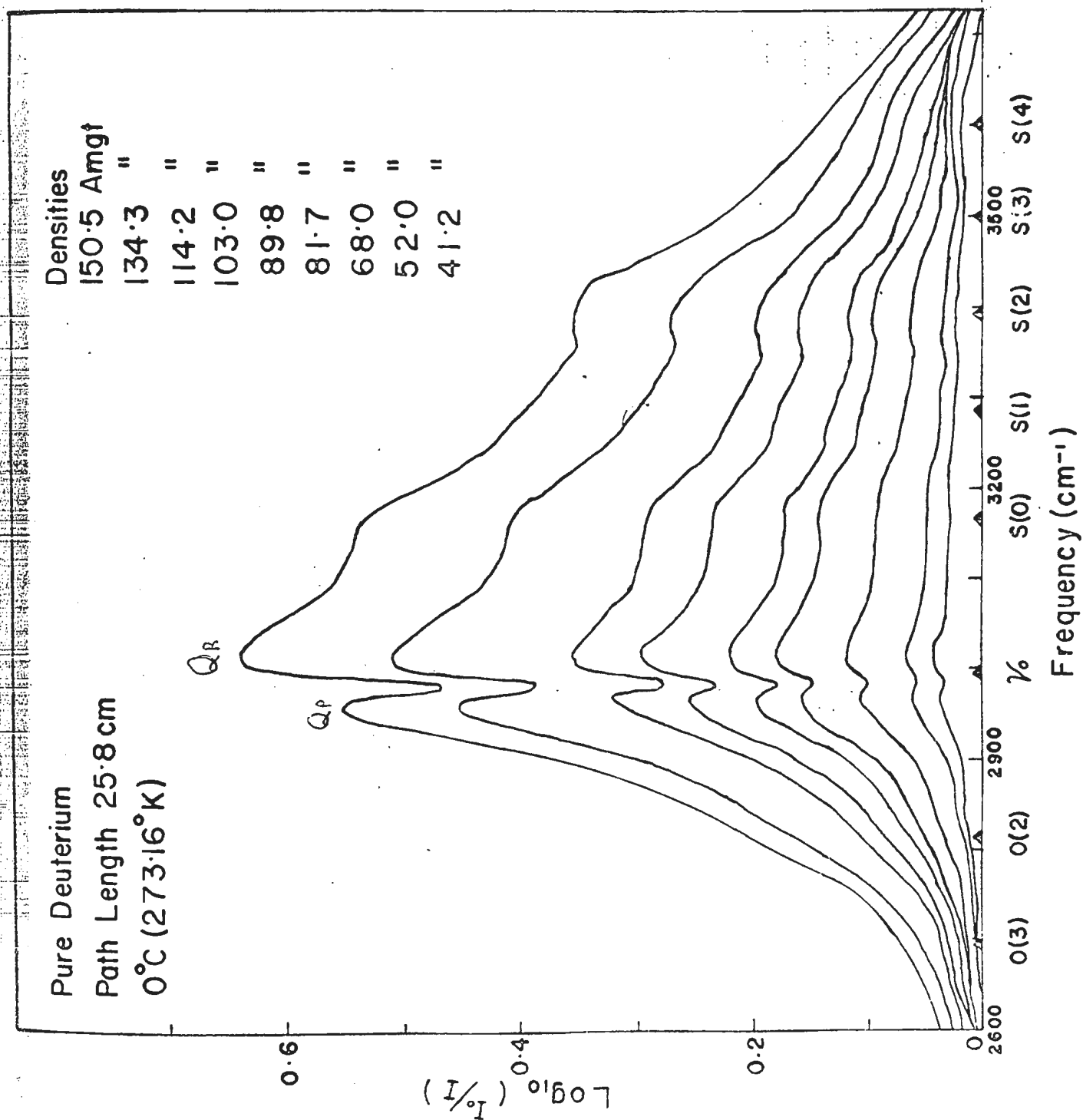
Perturbing gas	Temp °K	Optical path length, cm.	Max density Amt	No. of experiments
Deuterium	273.16	25.8	150.5	2
"	201.16	25.7	174.8	2
"	77.3	25.7	171.8	2

It is not intended in the present work to carry out a detailed contour-analysis of the induced fundamental band of deuterium. However, it may be mentioned here that a detailed analysis of the contours of the pressure-induced fundamental infrared absorption band of hydrogen was first carried out by Hunt and Welsh (1964). When such an analysis is done for the deuterium fundamental band, it will be possible to estimate the half-width of the Q branch, the half-widths of the S and O lines and the contribution of the double transitions in the S branch to the total absorption. In the following paragraphs, the main features of the contours of the fundamental band of deuterium obtained in this investigation are described qualitatively.

The main feature of the absorption contours at the ice-fixed point (273.16°K) is the splitting of the Q branch into two well resolved components with the minima occurring at the band origin, ν_0 . The higher and lower frequency components are often referred to as Q_R and Q_P respectively in accordance with the usual notation. A similar splitting of the Q branch in the fundamental band of deuterium at room temperature has been observed by Reddy and Cho (1965a). The separation of the Q_R and Q_P maxima in the deuterium fundamental band is observed to increase with density. The contours at the ice temperature also show pronounced S(0) and S(2) components with an indication of S(1) and O(2) components. It is seen from Fig. 7 that as the density of the gas is increased, the minima of the Q branch and the maxima of the Q_R component do not show appreciable shift in frequency while the maxima of the Q_P

LIBRARY

Fig.7. The observed pressure-induced fundamental vibration-rotation absorption band of pure deuterium at ice temp. (0°C) at a series of gas densities.



component does show a shift of 5 to 8 cm^{-1} towards lower frequency at higher densities.

The absorption profiles of the deuterium fundamental band at alcohol - dry ice temperature (Fig. 8) show the splitting of the Q branch into the Q_p and Q_R components just as those at ^{the} Λ ice-point. But the $S(0)$ and $S(1)$ components in these contours are more pronounced than the corresponding components at 0°C .

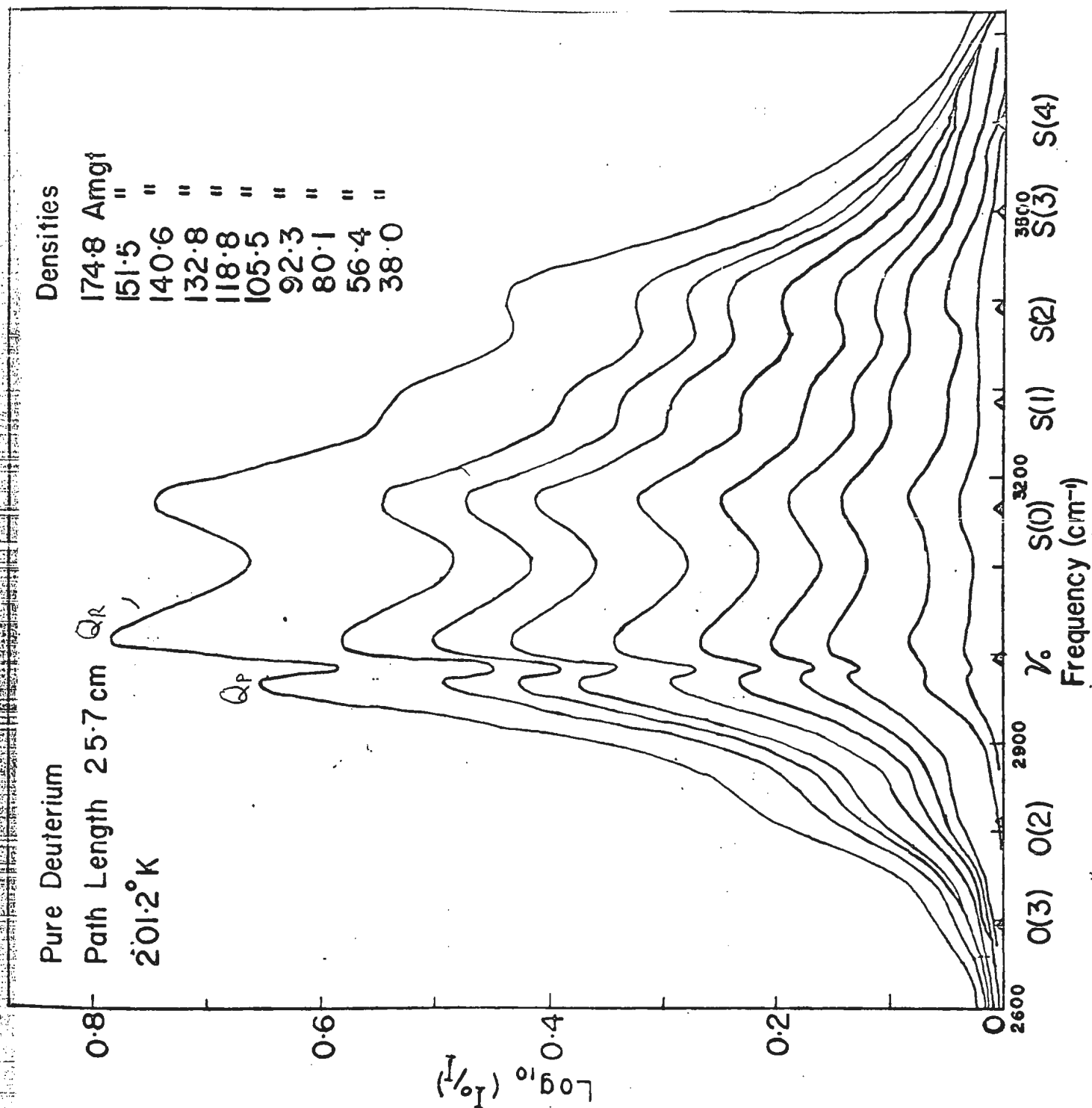
The absorption contours at liquid nitrogen temperature are distinct enough to show the marked effect of low temperature. The interesting features of these contours are described below:

(a) The splitting of the Q branch into higher and lower frequency components about the band origin, ν_0 , is not observed at lower densities. This was also reported recently by Watanabe and Welsh (1965) for deuterium contours at 68°K . But at higher densities, as seen in Fig. 9, the Q_R and Q_p components appear distinctly.

(b) The $S(0)$ line is the most pronounced in these contours (Fig. 9). The width of this line at half the intensity is found to be almost constant. Unlike in the contours at 0°C and -72°C , the peak of the $S(0)$ line in the contours at -195.8°C is much more intense than that of Q_R .

(c) With increasing density the $S(1)$ component becomes more pronounced and its maxima does not show any appreciable shift. Though the $S(2)$ component is feeble at low densities, it becomes distinct at higher densities. The $O(2)$ component is found to be almost disappearing.

Fig.8. The pressure-induced fundamental absorption band of pure deuterium at alcohol-dry ice temperature (-72°C) at a series of gas densities.



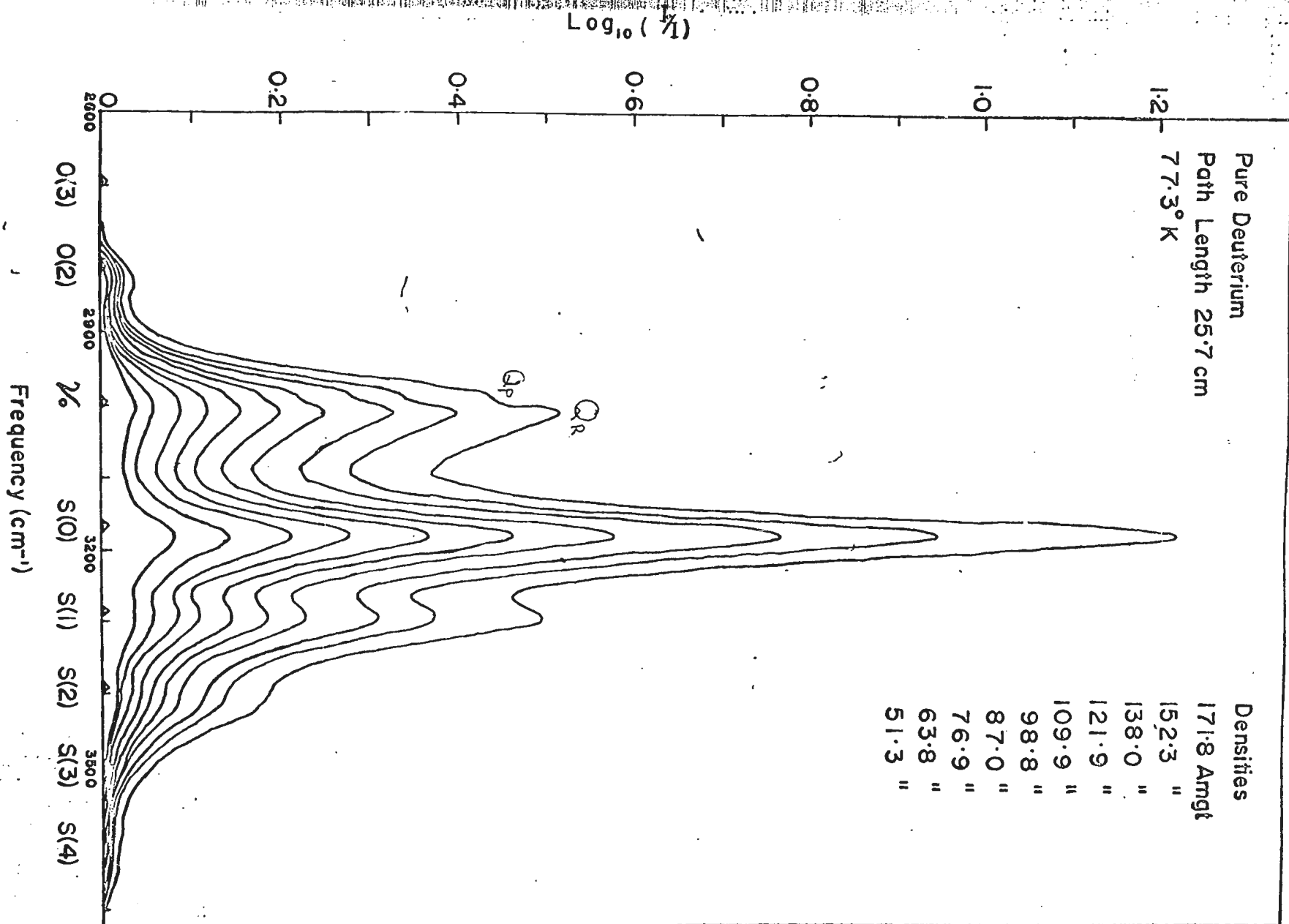


Fig.9. The pressure-induced fundamental absorption band of pure deuterium at liquid nitrogen temp. (-195.8°C) at a series of gas densities.

(ii) The Absorption Coefficients:

The values of the integrated absorption coefficient per unit path length, $\int \alpha(\nu) d\nu$ in cm^{-1}/cm , were calculated from the areas under the absorption profiles. They are summarized in Tables V(a), V(b) and V(c) for ice, alcohol - dry ice and liquid nitrogen temperatures respectively. The dependence of $\int \alpha d\nu$ on the density of deuterium, in Amagat units has been ascertained by plotting the quantity $(1/\rho_a^2) (\int \alpha(\nu) d\nu)$ vs ρ_a , where ρ_a is the density of pure deuterium gas, i.e. ρ_D . These plots represent almost straight lines with positive slopes.

The straight lines shown in Fig. 10 at various low temperatures have been obtained by the least squares fit. Thus, it may be concluded that ^{the} integrated absorption coefficient in the density range used in the present investigation can be represented by the equation,

$$(6) \quad \int \alpha(\nu) d\nu = \alpha_{1a} \rho_D^2 + \alpha_{2a} \rho_D^2$$

where α_{1a} and α_{2a} are the binary and ternary absorption coefficients of the gas component "a" respectively. Here, "a" refers to ^{the} pure deuterium gas component. The observed binary and ternary absorption coefficients, α_{1a} and α_{2a} , of deuterium gas at ice, alcohol - dry ice and liquid nitrogen temperatures, obtained by the least squares fit are summarized in Table IV, and the ranges of errors given are the standard deviations. For the purpose of comparison, α_{1a} and α_{2a} for deuterium at room temperature obtained by Reddy and Cho (1965) and α_{1a} at room temperature obtained by Chisholm (1952) are also presented in Table VI.

TABLE V(a)

Summary of results

Pure deuterium at ice temperature (0°C)

ρ_D (Amgt)	f_{adv} (cm ⁻¹ /cm)	ρ_D (Amgt)	f_{adv} (cm ⁻¹ /cm)
41.10	1.92	73.40	6.50
51.70	3.11	87.60	9.50
68.00	5.55	97.60	11.93
81.65	8.23	106.50	14.63
89.80	10.10	119.50	18.82
102.80	13.61	125.00	20.79
114.15	17.10	130.50	22.85
134.30	24.39	139.00	26.19
150.45	31.52	-	-
42.70	2.06	-	-
57.70	3.89	-	-

TABLE V(b)

Summary of results

Pure deuterium at alcohol - dry ice temperature (-72°C)

ρ_D (Amt)	f_{adv} (cm^{-1}/cm)	ρ_D (Amt)	f_{adv} (cm^{-1}/cm)
38.06	1.42	36.36	1.28
56.60	3.24	53.90	2.91
80.20	6.71	71.10	5.21
92.40	9.09	88.70	8.27
105.50	11.87	100.50	10.81
118.80	15.44	113.40	13.98
132.75	19.70	125.70	17.45
140.80	22.50	130.70	18.99
151.70	26.36	136.70	20.90
167.40	32.47	145.40	23.92
174.80	35.74	158.00	28.70

TABLE V(c)

Summary of results

Pure deuterium at liquid nitrogen temperature (-195.8°C)

ρ_D (Amgt)	f_{adv} (cm^{-1}/cm)	ρ_D (Amgt)	f_{adv} (cm^{-1}/cm)
39.26	0.98	33.24	0.69
56.61	2.08	51.29	1.69
69.63	3.24	63.82	2.68
81.17	4.51	76.85	3.98
93.46	6.13	86.98	5.26
104.07	7.77	98.77	6.82
120.00	10.51	109.85	8.68
127.00	11.98	121.88	10.88
136.57	14.04	129.10	12.32
148.86	16.96	138.03	14.35
167.41	22.04	152.26	17.64
-	-	171.76	23.33

- 41 -

Fig. 10. The relations between the integrated absorption coefficients and densities of normal deuterium at various low temperatures.

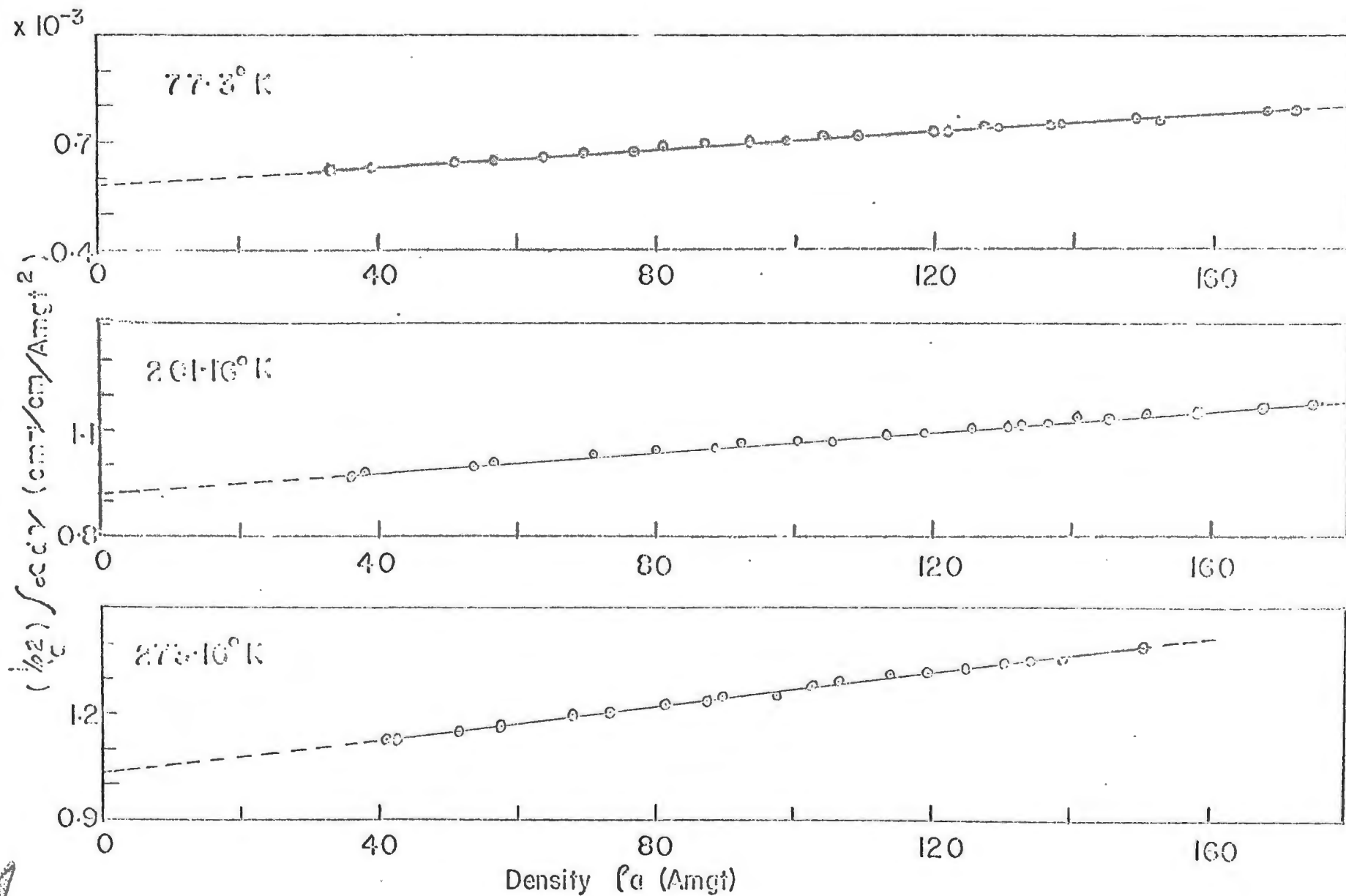


TABLE VI

Observed absorption coefficients of the induced fundamental band
of deuterium in the pure gas at various temperatures†

Temperature °K	Binary Absorption Coefficient		Ternary Absorption Coefficient (10 ⁻⁶ cm ⁻² Amgt ⁻³)
	(10 ⁻³ cm ⁻² Amgt ⁻²)	(10 ⁻³⁵ cm ⁶ sec ⁻¹)	
273.16	$\alpha_{1a} = 1.032 \pm 0.003$	$\tilde{\alpha}_{1a} = 1.365$	$\alpha_{2a} = 2.39 \pm 0.03$
201.16	$\alpha_{1a} = 0.926 \pm 0.003$	$\tilde{\alpha}_{1a} = 1.225$	$\alpha_{2a} = 1.42 \pm 0.03$
77.3	$\alpha_{1a} = 0.584 \pm 0.002$	$\tilde{\alpha}_{1a} = 0.765$	$\alpha_{2a} = 1.21 \pm 0.02$
298	$^*\alpha_{1a} = 1.06 \pm 0.02$	$^*\tilde{\alpha}_{1a} = 1.402$	$^*\alpha_{2a} = 0.80 \pm 0.20$
298	$^{**}\alpha_{1a} = 1.10$	$\tilde{\alpha}_{1a} = 1.455$	

*Value obtained by Reddy and Cho (1965)

**Value obtained by Chisholm (1952)

†The ranges of errors in the values of α_{1a} and α_{2a} quoted here are standard deviations. They do not include the experimental errors which may be up to 2%.

For comparison with theory the binary absorption coefficient is expressed in the form:

$$(7) \quad \tilde{\alpha}_1 = \frac{c\alpha_1}{n_0^2 \bar{\nu}}$$

where $\tilde{\alpha}_1$ and α_1 are the binary absorption coefficients in units $\text{cm}^6\text{sec}^{-1}$ and $\text{cm}^{-2} \text{Amgt}^{-2}$ respectively, $\bar{\nu}$ is the mean frequency of the band, c is the velocity of light, and n_0 is the Loschmidt's number, defined as $n_0 = N/V_0$, N , being Avogadro's number and V_0 , being the gram-molecular volume at N.T.P. In equation (7), the absorption frequency factor is removed, so that $\tilde{\alpha}_1$ (in $\text{cm}^6 \text{sec}^{-1}$) is actually the transition probability. The values of α_{1a} (in $\text{cm}^{-2} \text{Amgt}^{-2}$) and of the corresponding $\tilde{\alpha}_{1a}$ (in $\text{cm}^6 \text{sec}^{-1}$) are presented in Table VI. $\bar{\nu}$ for deuterium at ice, alcohol - dry ice, and liquid nitrogen temperatures are found to be 3140 cm^{-1} , 3141 cm^{-1} and 3171 cm^{-1} respectively.

(iii) Discussion.

In Fig. 11 the absorption contours of the pure deuterium gas at approximately equal densities at different temperatures have been compared and the following points noted:

(a) Transitions with $\Delta J = 0$ (where J is the rotational quantum number) induced by the overlap interaction account for the major part of the intensity of the Q branch in the induced fundamental bands. The splitting of the Q branch into Q_R and Q_P components has been interpreted as due to the summation and difference tones respectively, of the vibrational frequency, ν_0 , of the deuterium molecule with the continuum of frequencies due to the kinetic motions of the molecules during the collision.

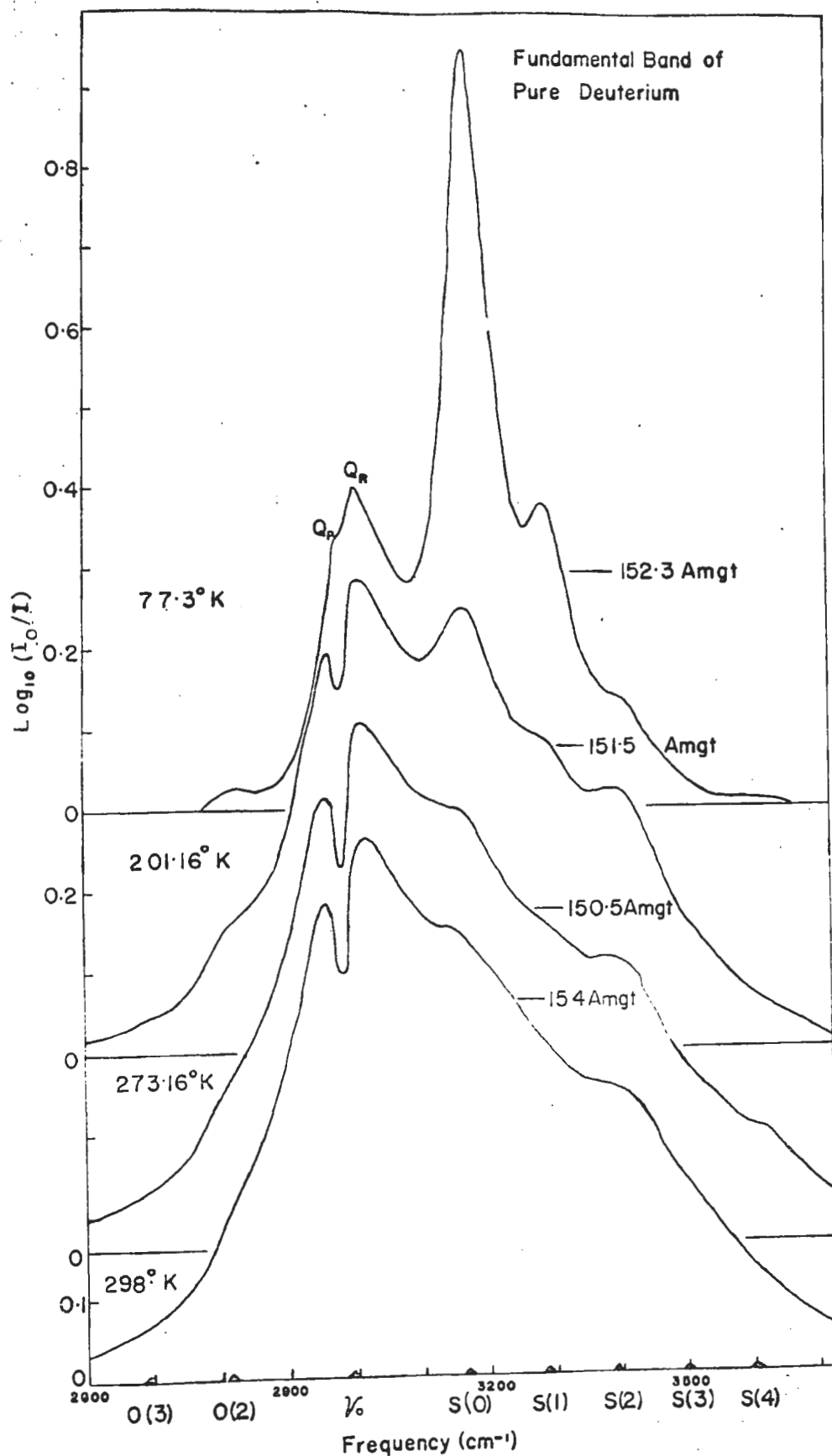


Fig. 11. Absorption contours of the pressure-induced fundamental band of pure deuterium at various temperatures.

(b) The intensity of the Q branch at constant density is seen to be decreasing with decreasing temperature.

(c) The magnitude of the splitting of the Q branch at constant density decreases as the temperature is lowered. The splitting disappears completely at liquid nitrogen temperature (77.3°K) in the low density region, which has been also observed by Watanabe and Welsh (1965) for deuterium gas at 68°K. Although the minima between the Q_P and Q_R components is in all cases at the band origin, ν_0 , the depth becomes smaller as the temperature is lowered. At low temperatures and low densities, the gas molecules have less kinetic energy. Therefore, the difference and summation tones fall very close to the vibrational frequency ν_0 and the Q_P and Q_R components are not resolved.

(d) The reappearance of the splitting of the Q branch at higher densities at liquid nitrogen temperature and also the increased splitting in general at higher densities for all temperatures considered here, are easily understood as a consequence of the participation of the increased kinetic energy in the absorption process. Since the splitting increases linearly with the density, it must involve ternary collisions, the absorption itself is caused by a two-body collision and any feature of absorption varying with density has to be ascribed to an interaction with the third molecule. A similar interpretation has been made by Chisholm and Welsh (1954).

(e) The transition with $\Delta J = 0$ induced by quadrupole interaction has been designated as ^{the} Λ_Q component of the vibrational band,

W. J. N. LIBRARY

which has not been observed for deuterium gas in the present investigation.

(f) $\Delta J = +2$ transitions due to quadrupolar interaction contribute to the intensity of the S branch. Since the duration of collision is greater at low temperature, the absorption lines are much sharper in the low temperature range. Though there is not much difference in the absorption peaks at room and ice temperatures, the S(0) and S(2) lines are sharper at alcohol-dry ice temperature (201.2°K), whereas the S(0) and S(1) lines become much sharper at liquid nitrogen temperature (77.3°K). Since the S(0) maxima become comparable to the Q_R maxima at alcohol-dry ice temperature, it is expected that as the temperature is lowered the S(0) maxima rise very rapidly while the Q_R maxima and its extent towards higher frequency decreases rapidly so that the intensity ratio $S(0)_{\max} / Q_{R\max} = 2.38$ approximately at 77.3°K compared to the corresponding ratio $S(0)_{\max} / Q_{R\max}$ which is less than 1 at 201.2°K.

(g) Due to the depopulation of the higher rotational levels at liquid nitrogen temperature, the S(2) lines become very feeble. The transitions $\Delta J = +2$ due to interaction in the region of overlap forces contribute very little to the S-line intensity when the polarizability of the perturbing molecule is small as pointed out by Kiss et al (1959).

(h) Because of the reason given in (g) above, the O branch lines (i.e. $\Delta J = -2$) almost disappear at liquid nitrogen temperature.

AM. U. N. LIBRARY



(i) In general, the overall width of the band decreases with decreasing temperature, which is caused not only by the decreasing line width but also by the depopulation of the higher rotational levels at low temperature.

A survey of the observed binary absorption coefficients at various temperatures, summarized in Table VI shows a decreasing trend in the values of the binary absorption coefficients for deuterium as the temperature is lowered. A qualitative comparison of the theoretical and experimental variation of the binary absorption coefficient of deuterium gas with temperature will appear in Chapter V of this thesis.

4.2 Deuterium-foreign gas mixtures at 77.3°K.

(i) The Absorption Profiles:

Table IV(b) below summarizes the experimental conditions for which enhancement absorption contours of the fundamental band of deuterium in D₂-foreign gas mixtures have been studied.

TABLE IV(b)

Outline of the experiments

Perturbing gas	Temperature °K	Optical path length, cm	Max density Amt.	No. of experiments
D ₂ + Helium	77.3	25.7	697.3	2
D ₂ + Neon	77.3	25.7	453.3	2

M. U. N. LIBRARY

In Figs. 12 and 13, a set of enhancement profiles of the induced fundamental band of deuterium in D_2 -He mixtures (at liquid nitrogen temperature) with fixed base densities of deuterium as 59.7 Amgt and 46.6 Amgt respectively are presented at a series of partial densities of helium. The main feature of these contours is the splitting of the Q branch into two well resolved components Q_R and Q_P with the minima occurring at the band origin, ν_0 . The minima between the Q_P and Q_R components show no appreciable change with the density of the mixture except at very low densities, where the minima drops down a little. The difference between the intensities of the $(Q_P)_{\max}$ and the $(Q_R)_{\max}$ increases very rapidly with increasing density of the mixture. There is no indication of the appearance of any absorption peaks corresponding to the S and O lines. The contours for D_2 -He mixtures at 77.3°K are very similar to the corresponding contours at room temperature obtained by Pai, Reddy and Cho (1966), except for the fact that the widths of the Q branch peaks are narrower at low temperature.

Figs. 14 and 15 represent the sets of the observed enhancement profiles of the fundamental band of deuterium in deuterium-neon mixtures at liquid nitrogen temperature for the fixed base densities of deuterium, 61.0 and 53.2 Amgt respectively. These contours show markedly several absorption peaks agreeing well with the calculated positions of the S lines, in addition to the most prominent Q_P and Q_R peaks similar to those of the deuterium-helium mixtures. While the S(0) peak is well resolved at higher densities of the mixture the

Fig.12. The observed pressure-induced fundamental vibration-rotation absorption band of deuterium in deuterium-helium mixture at liquid nitrogen temperature (77.3°) at a series of foreign gas densities.

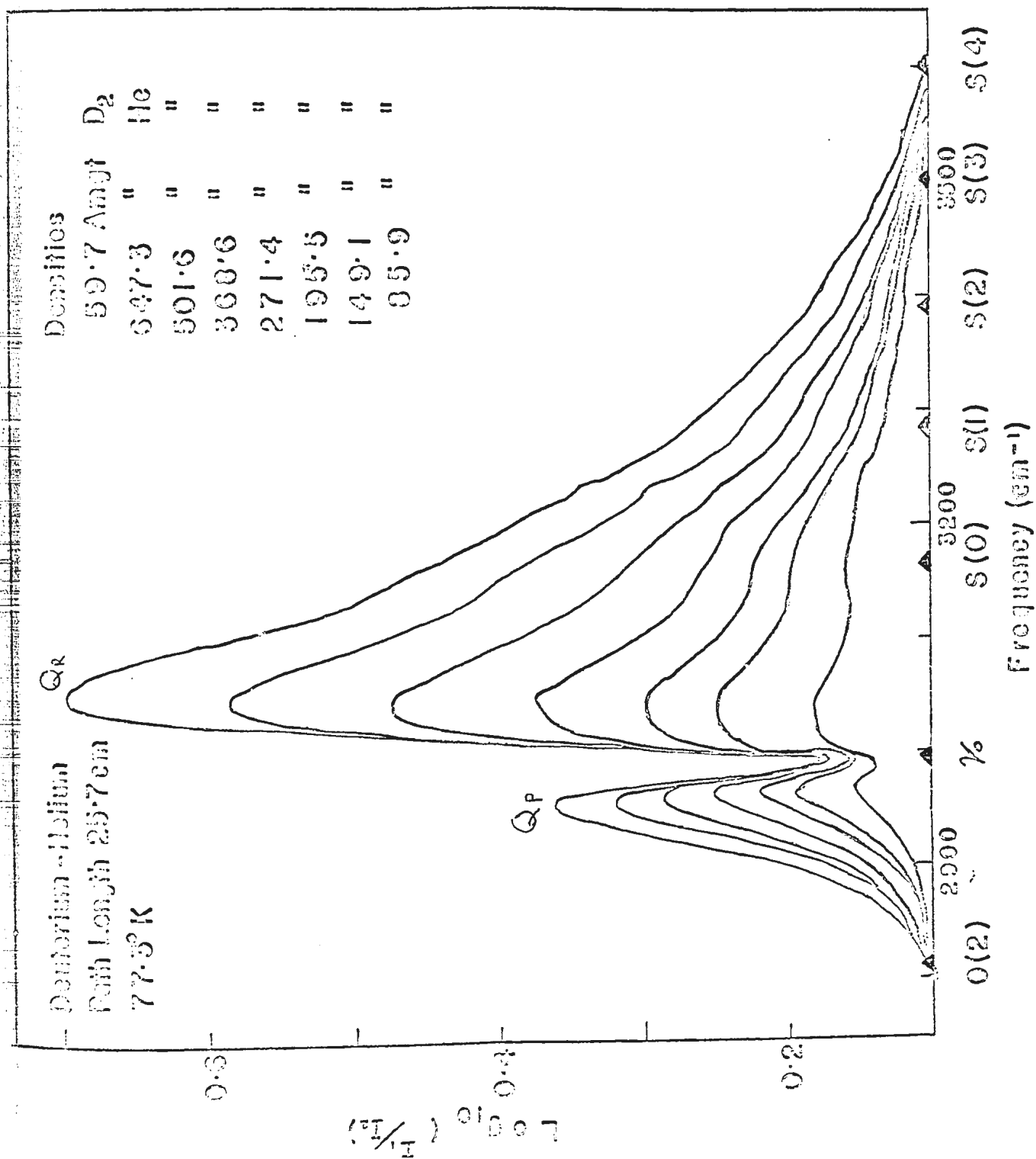


Fig. 13. The pressure-induced fundamental absorption band of deuterium in deuterium-helium mixture at 77.3°K at a series of foreign gas densities.

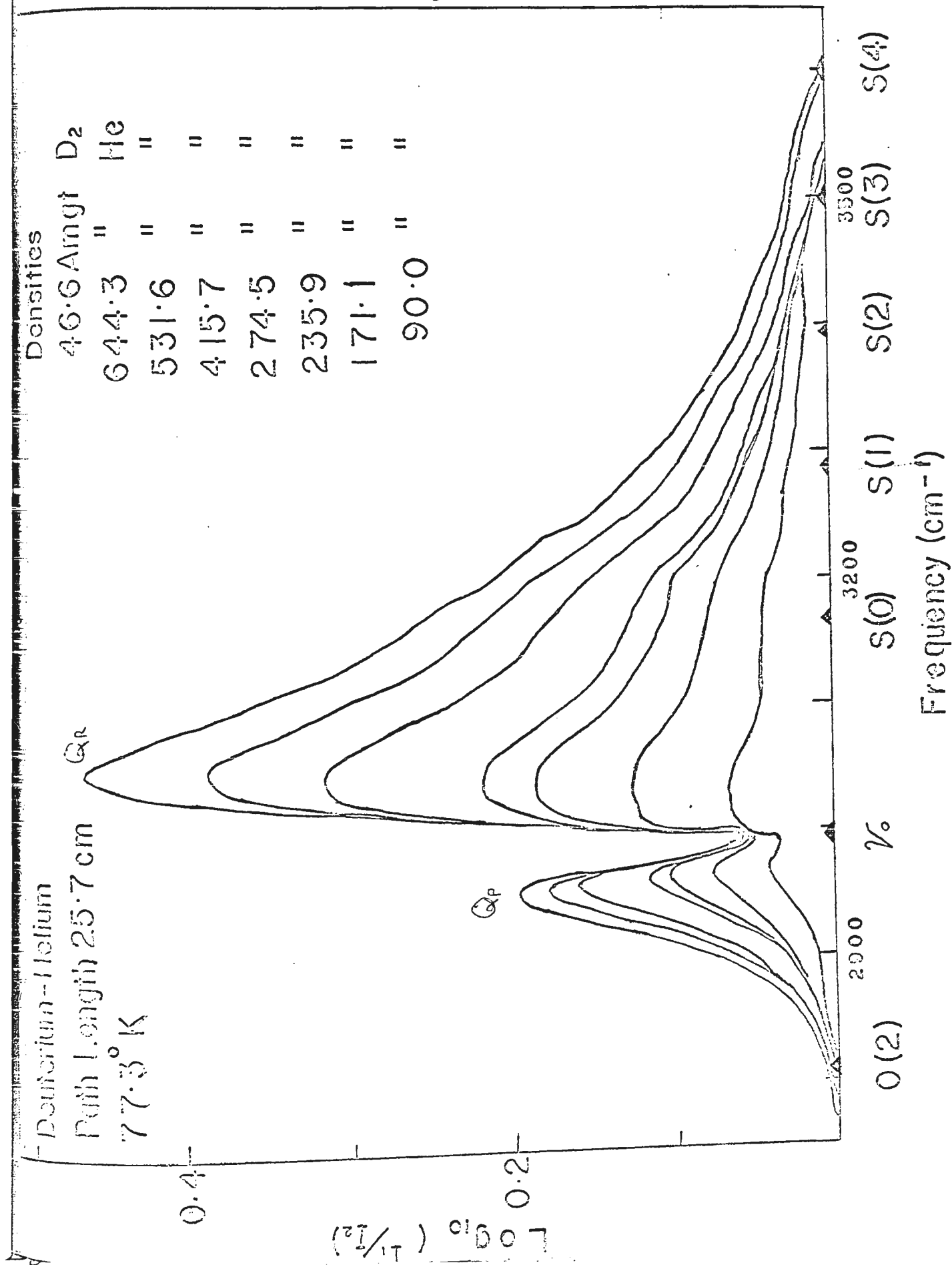


Fig.14. The observed pressure-induced fundamental vibration-rotation absorption band of deuterium in deuterium-neon mixture at 77.3°K at a series of foreign gas densities.

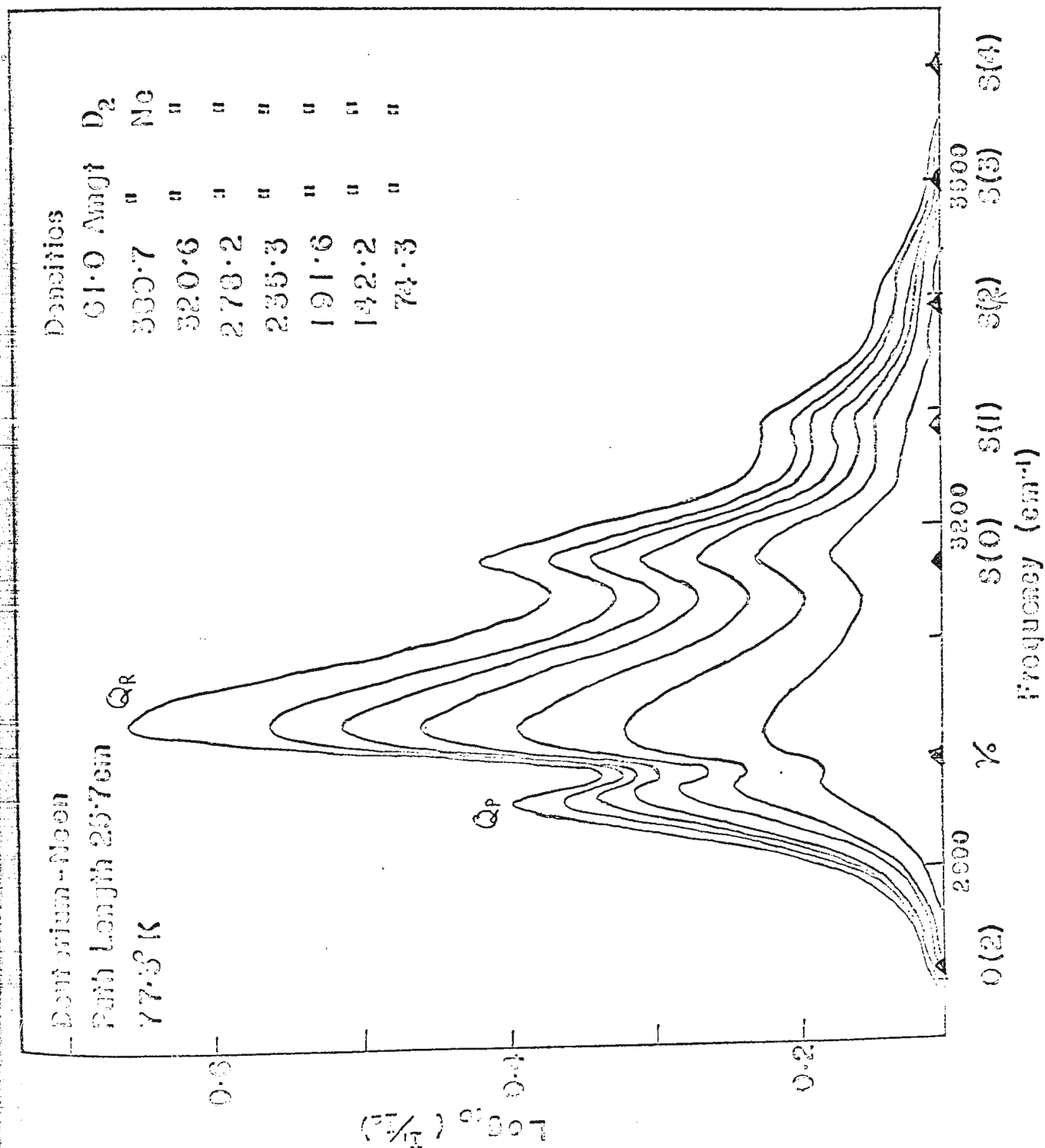
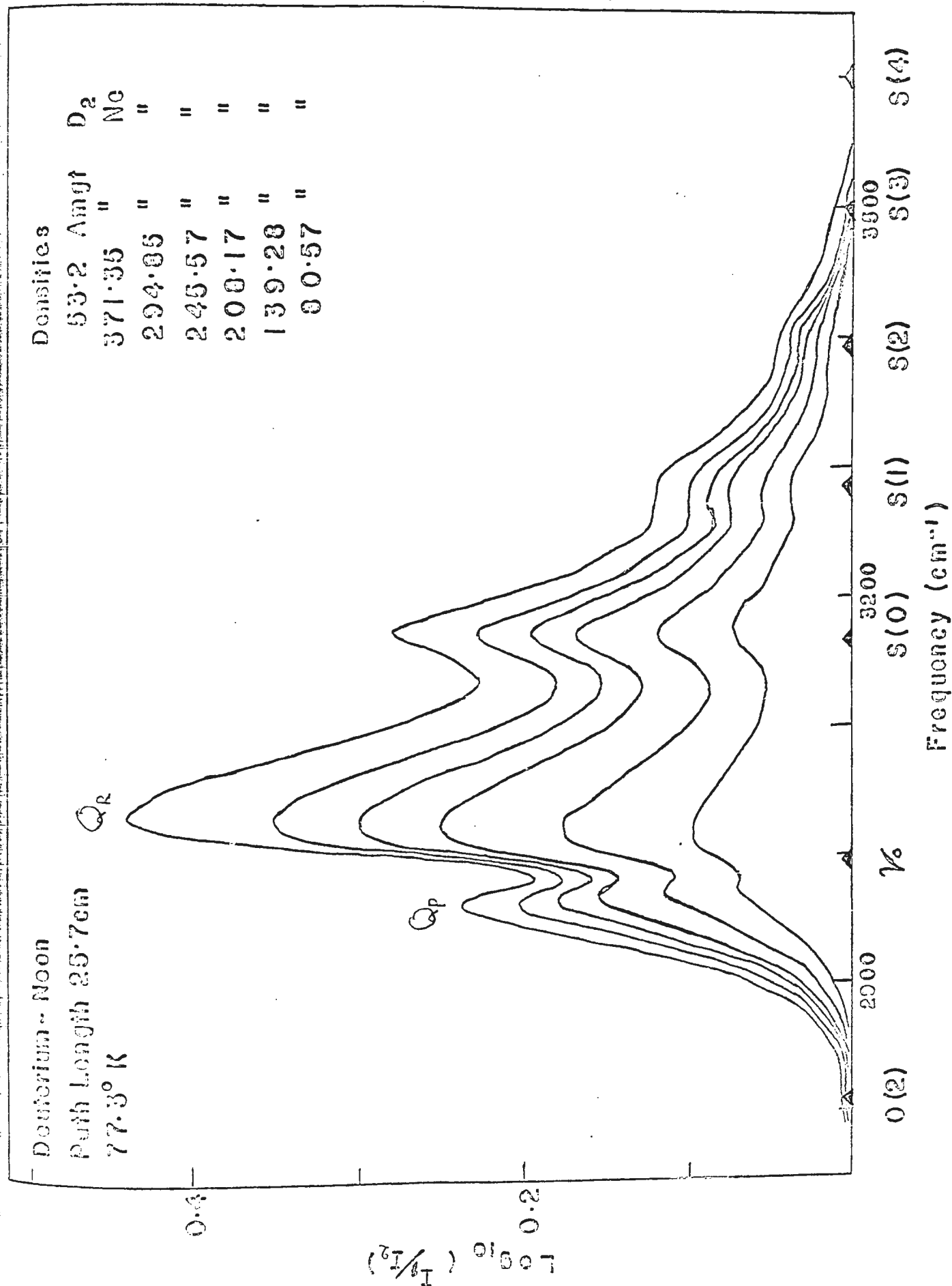


Fig.15. The pressure-induced fundamental absorption band of deuterium in deuterium-neon mixture at 77.3°K at a series of foreign gas densities.



S(1) peak is not resolved well but ^{is} quite distinct. There is an indication of the S(2) line but not the 0 branch. The minima between the $(Q_P)_{\max}$ and the $(Q_R)_{\max}$ occurring at the band origin, ν_0 , show much dependence on the density of the mixture and rise higher with the increasing density, in contrast with the contours of D₂-He mixtures.

(ii) The Absorption Coefficients:

The observed enhancements in the integrated absorption coefficients of the fundamental band of deuterium in deuterium-foreign gas mixtures at liquid nitrogen temperature are summarized in Tables VII and VIII for D₂-He and D₂-Ne respectively. The quantity $(1/\rho_a \rho_b) \times (\int_{\text{enh}} \alpha(\nu) d\nu)$ when plotted against ρ_b gave almost straight lines with negative slopes as shown in Fig. 16 where the straight lines were obtained by linear least squares fit. Here, "a" refers to the base deuterium gas (D₂) and "b" refers to the foreign gas. Thus, one may conclude that enhancement integrated absorption coefficient can be expressed (in the density region studied here) as,

$$(8) \quad \int_{\text{enh}} \alpha(\nu) d\nu = \alpha_{1b} \rho_a \rho_b + \alpha_{2b} \rho_a \rho_b^2,$$

where α_{1b} and α_{2b} are the enhancement binary and ternary absorption coefficients respectively of ^{the} deuterium fundamental band in D₂-foreign gas mixtures. The observed α_{1b} and α_{2b} and the range of error obtained by ^a linear least squares method, are presented in Table IX. For the purpose of comparison, the α_{1b} value for D₂-He at room temperature, obtained by Pai, Reddy and Cho (1966), is also presented in the same

TABLE VII

Summary of results

D₂-He mixture at liquid nitrogen temperature

ρ_{D_2} (A _{mg} t)	ρ_{He} (A _{mg} t)	f_{adv}^{enh} (cm ⁻¹ /cm)
59.70	85.87	2.16
"	149.11	3.68
"	195.53	4.67
"	271.36	6.35
"	319.43	7.25
"	368.60	8.27
"	424.29	9.36
"	501.61	10.59
"	592.96	12.12
"	647.28	13.16
46.62	90.02	1.76
"	171.07	3.26
"	235.92	4.38
"	274.53	4.97
"	345.02	6.05
"	415.68	6.92
"	449.43	7.56
"	531.64	8.44
"	581.05	9.17
"	644.26	9.95

TABLE VIII

Summary of results

D₂-Ne mixture at liquid nitrogen temperature

ρ_{D_2} (Amgt)	ρ_{Ne} (Amgt)	$\int_{enh}^{\rho dv}$ (cm ⁻¹ /cm)
61.00	74.31	2.39
"	142.24	4.37
"	191.56	5.76
"	235.34	7.23
"	278.22	8.45
"	320.56	9.39
"	363.17	10.47
"	389.74	11.22
53.20	80.57	2.28
"	139.28	3.83
"	208.17	5.52
"	245.57	6.51
"	294.85	7.65
"	341.71	8.69
"	371.35	9.39

Fig.16. The relations between the enhancement integrated absorption coefficients of the fundamental band of deuterium and the partial densities of foreign gases in deuterium-foreign gas mixtures at liquid nitrogen temperature (77.3°K).

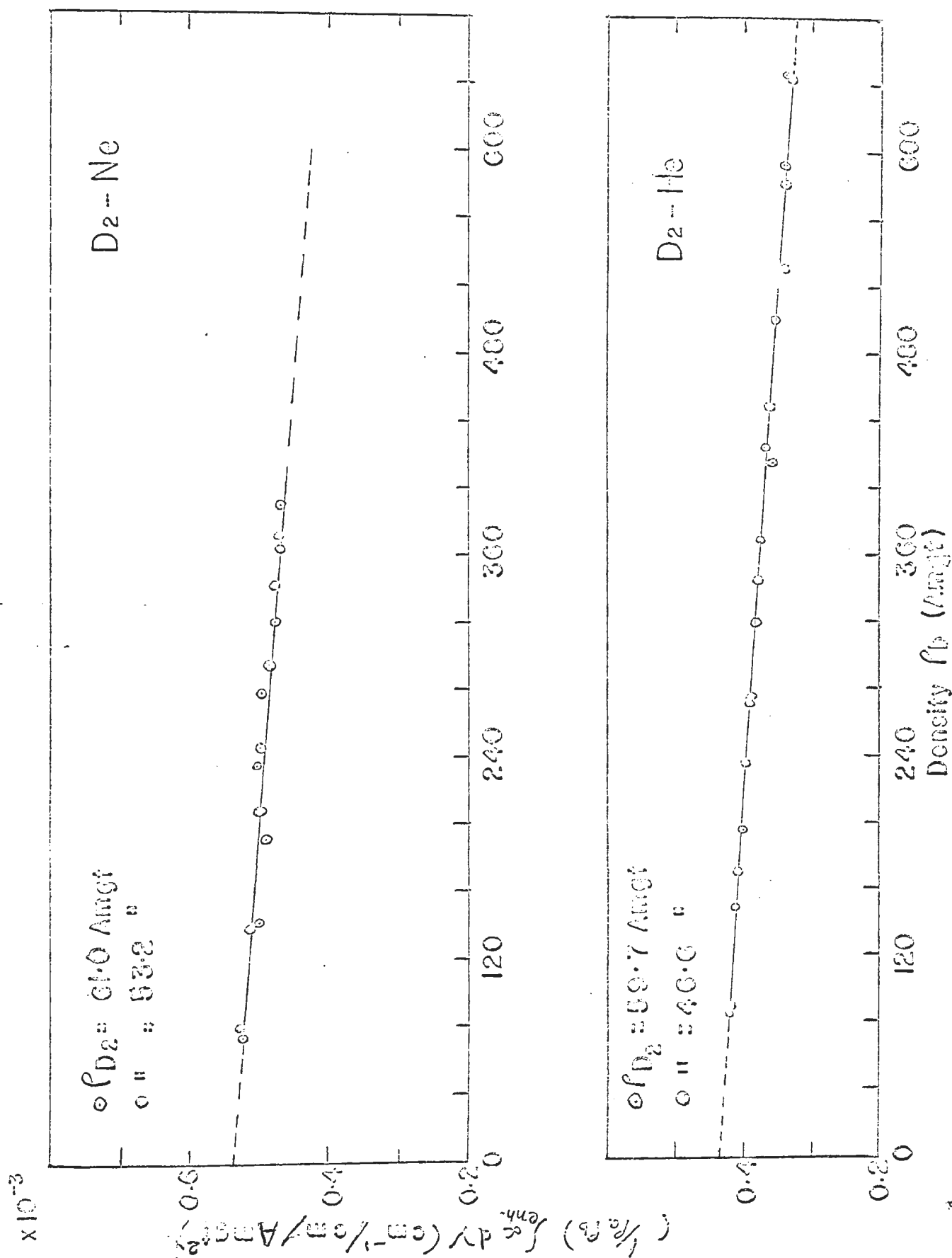


TABLE IX

Observed enhancement absorption coefficient of the induced fundamental
band of deuterium in deuterium-foreign gas mixtures†

Temperature (°K)	Mixture	Binary Absorption Coefficient		Ternary Absorption Coefficient
		(10 ⁻³ cm ⁻² Amgt ⁻²)	(10 ⁻³⁵ cm ⁶ sec ⁻¹)	
77.3	D ₂ -He	$\alpha_{1b} = 0.434 \pm 0.002$	$\alpha_{1b} = 0.579$	$\alpha_{2b} = -0.159 \pm 0.006$
77.3	D ₂ -Ne	$\alpha_{1b} = 0.538 \pm 0.004$	$\alpha_{1b} = 0.722$	$\alpha_{2b} = -0.171 \pm 0.15$
298	*D ₂ -He	$\alpha_{1b} = 0.82 \pm 0.01$	$\alpha_{1b} = 1.08$	$\alpha_{2b} = +0.27 \pm 0.03$

*Value obtained by Pai, Reddy and Cho (1966)

†The ranges of errors in the values of α_{1a} and α_{2a} quoted here are standard deviations. They do not include the experimental errors which may be up to 2%.

table. Again $\tilde{\alpha}_{1b}$ in $\text{cm}^6 \text{sec}^{-1}$ has been obtained from α_{1b} in $\text{cm}^{-2} \text{Amgt}^{-2}$ by relation (7). The $\bar{\nu}$ for $\text{D}_2\text{-He}$ and $\text{D}_2\text{-Ne}$ at liquid nitrogen temperature are found to be 3116 cm^{-1} and 3095 cm^{-1} respectively.

(iii) Discussion:

For the purpose of comparison, the absorption contours of $\text{D}_2\text{-He}$, $\text{D}_2\text{-Ne}$ and $\text{D}_2\text{-D}_2$ at 77.3°K are presented collectively in Fig. 17 together with the contour of $\text{D}_2\text{-He}$ at room temperature, obtained by Pai, Reddy and Cho (1966). Contours in Fig. 17 were chosen in such a way that the product of partial densities ρ_a, ρ_b for deuterium-foreign gas mixtures and ρ_a^2 for pure deuterium are almost equal to each contour. Also the contours of $\text{D}_2\text{-He}$ and $\text{D}_2\text{-Ne}$ were chosen to represent almost the same base density of deuterium ($\sim 60 \text{ Amgt}$). The products of partial densities are kept almost constant as far as practicable in order to make an overall comparison of absorptions arising from the binary collisions between the molecules involved, which is based on the assumption that induced absorption is due to the dipole moment induced by the colliding pairs of molecules. It is evident from Fig. 17 that the total absorption decreases in the following order: $\text{D}_2\text{-He}$ at room temperature (298°K), $\text{D}_2\text{-D}_2$ at 77.3°K , $\text{D}_2\text{-Ne}$ and $\text{D}_2\text{-He}$ at liquid nitrogen temperature. There is no appreciable difference between the shapes of the absorption contours of $\text{D}_2\text{-He}$ at 298°K and $\text{D}_2\text{-He}$ at 77.3°K except for the effect of low temperature in the latter case. As the temperature is lowered, the line-widths of the individual lines become narrower, the intensity of the Q_p component drops rapidly and the intensity ratio, $(Q_R)_{\text{max}}/(Q_p)_{\text{max}}$ becomes larger.

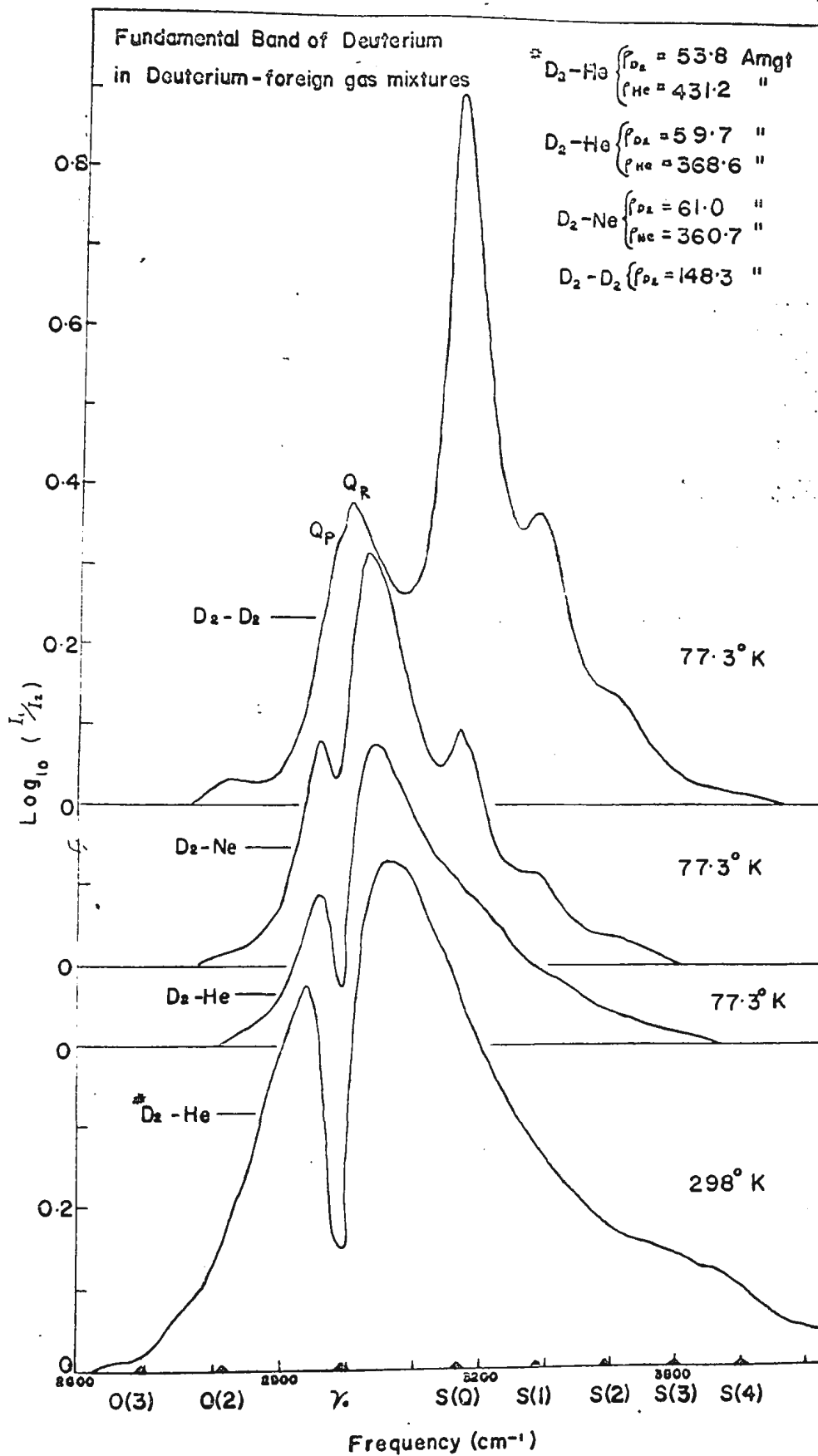


Fig.17. Absorption profiles of the pressure-induced fundamental band of deuterium for various perturbing molecules at various temperatures.

The contours of the fundamental band of deuterium in D_2 -He and D_2 -Ne mixtures at the liquid nitrogen temperature differ markedly from each other.

In D_2 -Ne contours the $S(0)$, $S(1)$ and $S(2)$ lines also appear and the depth of the minima between the Q_R and Q_P components increases with increasing density of the mixture. These features are not found in the contours obtained for D_2 -He mixtures. The Q_P component is relatively more intense for D_2 -Ne than for D_2 -He. This explains the shift of the mean frequency

of the fundamental band of deuterium in D_2 -Ne mixture towards the lower frequency side (3095 cm^{-1}).

There is not much difference between the shapes of the contours for pure D_2 and D_2 -Ne mixtures at liquid nitrogen temperature except for the basic fact that the Q branch is more prominent in D_2 -Ne mixtures with well resolved splitting into the Q_P and the Q_R components, whereas the S-branch is the most prominent in pure D_2 .

Ternary collisions in which the third molecule is in the region of Van der Waals forces are much more probable to give rise to the effect observed, although ternary collisions in the region of the overlap forces will not be significant except at very high densities. Classically, the presence of the third molecule makes large changes in the relative kinetic energy of the absorbing pair of molecules, because more kinetic energy is available for conserving the momentum readily. This effect should be greatest when the perturbing molecule is large and the Van der Waals forces have a long range. Thus, the splitting of the Q branch with neon as a foreign gas should increase more rapidly

with increasing density than the splitting with helium as a foreign gas. This is in accordance with the observations in the present investigation and is very similar to the observations of Chisholm and Welsh (1954).

A glance at the values of $\tilde{\alpha}_1$ for D_2 - D_2 , D_2 -Ne, D_2 -He at liquid nitrogen temperature reveals that the transition probability for absorption for D_2 -Ne and D_2 -He is approximately 94.4% and 75.7% respectively of that for D_2 - D_2 at liquid nitrogen temperature. In the case of D_2 -He at room temperature, the transition probability is 71.1% of that for pure D_2 at the same temperature.

The empirical relation given by equation (8) contains second order and third order terms in ρ_a and ρ_b . While the second order term, $\alpha_{1b}\rho_a\rho_b$ has been interpreted as the contribution arising from the binary collisions of the type a-b of the absorbing molecules a and the perturbing molecules b, to the enhancement absorption, the third order term, $\alpha_{2b}\rho_a\rho_b^2$, has been interpreted by previous authors as due to three ternary effects. These are (a) the finite volume effect (b) ternary collision and (c) the change of molecular polarizability with pressure.

Volume effect has been much discussed by Chisholm and Welsh (1954). Qualitative considerations have shown that ternary and higher order collisions would annul to some extent the contribution of the binary collisions to the absorption when a particular absorbing molecule is surrounded by a symmetrical configuration of the perturbing molecules. This is often referred to as "the cancellation effect". The decrease in molecular polarizabilities at high densities predicted by

quantum mechanical considerations (Michel, DeBoer, and Bijl, (1937), DeGroot and Tenseldom (1947)), would lower the absorption coefficient to some extent, but the magnitude of the effect (difficult to estimate) is probably very small at least for hydrogen gas.

It may be pointed out that another possible term $\alpha_{2ab} \rho_a^2 \rho_b$ is missing in equation (8), which is probably due to the limited experimental accuracy involved in the present results and also due to the smallness of ternary coefficients, α_{2b} .

As seen in Table IX, the ternary coefficients for mixtures D_2 -He and D_2 -Ne have negative values (i.e. negative slopes) at liquid nitrogen temperature, which indicate the predominance of the so-called "cancellation effect" over the other ternary collision effects, which has been explained at length by Hare and Welsh (1958), Van Kranendonk and Bird (1951), Van Kranendonk (1957, 1959).

The influence of the finite molecular volumes on the collision frequency and consequently on the coefficient of pressure-induced absorption has been estimated by Chisholm and Welsh (1954). Based on simple calculation they have derived the following expressions relating the absorption coefficients and the molecular diameter, D .

For ^{the} pure gas, the expression is given by

$$(9) \quad \alpha_{2a}/\alpha_{1a} = (8/9)\pi n_0 D_a^3$$

where D_a is the molecular diameter of ^{the} pure gas. The corresponding

expression for a mixture of two gases is,

$$(10) \quad \alpha_{2b}/\alpha_{1b} = (4/3)\pi n_o D_b^3$$

where D_b is the molecular diameter of the foreign gas molecule.

Using the observed values of α_{1a} and α_{2a} from Table VI for pure deuterium gas at 0°C (ice temperature), the molecular diameter of deuterium, D_a , was calculated and given in Table X. Similarly, using the observed values of α_{2b} and α_{1b} for D_2 -He and D_2 -Ne mixtures, values of the molecular diameters of helium and neon are calculated and presented in Table X. The corresponding values of σ , the distance of nearest approach of the two molecules colliding with zero initial kinetic energy are also presented in Table X for comparison.

It is seen that the present value of D for helium is better than that obtained by previous authors. Also the difference between the calculated values of D and ^{the} kinetic theory values increases in the following order: D_2 - D_2 , D_2 -He and D_2 -Ne. The probability of three-body collisions for heavier molecules is greater than for deuterium or helium since the range of the interaction forces is undoubtedly greater. This will make the difference in the calculated values of D and σ , larger for neon, smaller for helium and still smaller for deuterium as observed in the present investigation. A similar argument has been forwarded by Chisholm and Welsh (1954).

A better value obtained in this investigation is probably due to the fact that the experiments have been done at low temperatures

TABLE X

Molecular diameter of perturbing gas

Perturbing gas	<u>Molecular Diameter</u>		<u>Pai**</u>	<u>Chisholm and Welsh***</u>
	D	σ^*	D	D
	o (A)	o (A)	o (A)	o (A)
Deuterium	3.13	2.928	-	-
Helium	2.26	2.556	1.44	1.8
Neon	2.16	2.75	-	-

*Value obtained from "Molecular Theory of Gases and Liquids" by Hirschfelder, Curtis and Bird (1954).

**Value obtained by Pai (1965)

***Value obtained by Chisholm and Welsh (1954).

which decrease the kinetic energy effect, so that the probability of three-body collisions is relatively smaller when compared to that at higher temperatures. A little higher value of D for deuterium than the corresponding σ -value indicates the limited accuracy obtained in evaluating the slope of the straight line and extrapolating the straight line to zero density.

CHAPTER 5

THEORY* AND CALCULATIONS

5.1 The Theory of the Binary Absorption Coefficients;

The theory of the pressure-induced fundamental infrared absorption bands of homonuclear diatomic gases has been given by Van Kranendonk and Bird (1951), Van Kranendonk (1952, 57, 58) and Britton and Crawford (1958).

(i) Van Kranendonk's Expression for Binary Absorption Coefficients of^a Pure Gas:

According to the "exp-4 model" of Van Kranendonk (1957, 1958), the moment induced in a binary molecular collision can be separated into two additive parts: a short-range angle-independent overlap moment, of strength ξ and range ρ , which decreases exponentially with increasing intermolecular distance R ; and a long-range angle-dependent moment which is proportional to R^{-4} . The long-range moment is assumed to be dependent on the derivatives of the quadrupole moment and the average polarizability of the absorbing molecule, Q'_1 and α'_1 respectively, and the quadrupole moment and the average polarizability of the perturbing molecule, Q and α_2 respectively. For a pure gas both the absorbing and perturbing molecules are the same molecules. Here,

$$Q'_1 = (\partial Q_1 / \partial r_1)_0 \text{ and } \alpha'_1 = (\partial \alpha_1 / \partial r_1),$$

r_1 being the internuclear distance of the absorbing molecule. Based on

*The theory of Van Kranendonk has been summarized by Reddy and Cho (1965) and Pai et al (1966).

the above assumptions, Van Kranendonk (1958) has derived the following expressions for the binary absorption coefficients of the individual lines, with the rotational quantum number J , of the O, Q and S branches in an induced fundamental band:

$$(11) \quad \tilde{\alpha}_{1a}^{(0)} [O(J)] = (\mu_1^2 + \mu_2^2) \mathcal{J} \tilde{\gamma} \cdot P(J) \cdot L_2(J, J-2),$$

$$(12) \quad \tilde{\alpha}_{1a}^{(Q)} [Q(J)] = \lambda^2 \mathcal{I} \tilde{\gamma} \cdot P(J) \cdot L_0(J, J) + \mu^2 \mathcal{J} \tilde{\gamma} \cdot P(J) \times \\ \times L_2(J, J) + \mu_2^2 \mathcal{J} \tilde{\gamma} \cdot P(J) \cdot L_0(J, J) \times \\ \times \{ \Sigma_{J'} P(J') \cdot L_2(J', J') \},$$

$$(13) \quad \tilde{\alpha}_{1a}^{(S)} [S(J)] = (\mu_1^2 + \mu_2^2) \mathcal{J} \tilde{\gamma} \cdot P(J) \cdot L_2(J, J+2).$$

Here, the dimensionless parameters λ , μ_1 , μ_2 are defined as

$$(14) \quad \lambda = (\xi/e) \exp(-\sigma/\rho),$$

$$(15) \quad \mu_1 = Q_1 \alpha_2 / e \sigma^4, \quad \mu_2 = \alpha_1 Q_2 / e \sigma^4,$$

where σ is the intermolecular distance R for which the intermolecular potential is zero and e is the absolute value of the electronic charge.

The significance of λ is that λe represents the amplitude of the oscillating overlap dipole moment where the molecules are a distance σ apart. Similarly, $\mu_1 e$ and $\mu_2 e$ represent the amplitude of the quadrupole moment. $\tilde{\gamma}$ is defined as

$$(16) \quad \tilde{\gamma} = \pi e^2 \sigma^3 / 3 m_0 v_0,$$

where m_0 and v_0 are the reduced mass of the molecule and the frequency of the molecular oscillation respectively. The radial distribution integrals \mathcal{I} and

\mathcal{J} are given by

$$(17) \quad \mathcal{I} = 4\pi \int_0^{\infty} \exp \{ -2(x-1)\sigma/\rho \} g_0(x) x^2 dx$$

and

$$(18) \quad \mathcal{J} = 12\pi \int_0^{\infty} x^{-8} g_0(x) x^2 dx ,$$

where $x = R/\sigma$, and $g_0(x)$ is the low-density limit of the pair distribution function. In the equations (11), (12), and (13), $P(J)$ is the Boltzmann factor for the rotational level J , normalized in such a way that

$$\sum_J (2J + 1) P(J) = 1.$$

The quantities $L_0(J, J)$, $L_2(J, J-2)$, $L_2(J, J)$, and $L_2(J, J+2)$ are Racah coefficients (1942, 1943) which are given by

$$(19) \quad L_0(J, J) = 2J + 1,$$

$$(20) \quad L_2(J, J-2) = 3(J-1) J/2(2J-1),$$

$$(21) \quad L_2(J, J) = J(J+1)(2J+1)/(2J-1)(2J+3),$$

$$(22) \quad L_2(J, J+2) = 3(J+1)(J+2)/2(2J+3),$$

respectively. The total binary absorption coefficient, $\tilde{\alpha}_{1a}$, is obtained by adding (11), (12) and (13), after the summation over J . Thus,

$$(23) \quad \tilde{\alpha}_{1a} = \lambda^2 \mathcal{I} \tilde{\gamma} + (\mu_1^2 + \mu_1'^2) \mathcal{J} \tilde{\gamma}$$

(ii) The Enhancement Binary Absorption Coefficients of Gas Mixtures:

Considering the absorption by symmetrical diatomic molecules "a" induced by symmetrical diatomic foreign molecules, "b", Van Kranendonk (1958) has derived the following expressions for the enhancement binary absorption coefficients of the individual lines with the rotational quantum number J, of the O, Q, and S branches in the induced fundamental band:

$$(24) \quad \tilde{\alpha}_{1b}[O(J)] = \mu_1^2 \mathcal{J} \tilde{\gamma} \cdot P_a(J) \cdot L_2(J, J-2),$$

$$(25) \quad \tilde{\alpha}_{1b}[Q(J)] = (\lambda^2 \mathcal{I} + \mu_2^2 \mathcal{J}) \tilde{\gamma} \cdot P_a(J) \cdot L_0(J, J) \\ + \mu_1^2 \mathcal{J} \tilde{\gamma} \cdot P_a(J) \cdot L_2(J, J),$$

$$(26) \quad \tilde{\alpha}_{1b}[S(J)] = \mu_1^2 \mathcal{J} \tilde{\gamma} \cdot P_a(J) \cdot L_2(J, J+2).$$

When the "b" molecules are monatomic, $\lambda_2 = \mu_2 = 0$. The corresponding expressions are obtained as follows:

$$(27) \quad \tilde{\alpha}_{1b}[O(J)] = \mu_1^2 \mathcal{J} \tilde{\gamma} \cdot P_a(J) \cdot L_2(J, J-2),$$

$$(28) \quad \tilde{\alpha}_{1b}[Q(J)] = \lambda_1^2 \mathcal{I} \tilde{\gamma} \cdot P_a(J) \cdot L_0(J, J) \\ + \mu_1^2 \mathcal{J} \tilde{\gamma} \cdot P_a(J) \cdot L_2(J, J),$$

$$(29) \quad \tilde{\alpha}_{1b}[S(J)] = \mu_1^2 \mathcal{J} \tilde{\gamma} \cdot P_a(J) \cdot L_2(J, J+2).$$

Finally, by adding equations (27), (28) and (29) after summation over J, one will obtain the expression:

$$(30) \quad \tilde{\alpha}_{1b} = \lambda^2 \mathcal{I} \tilde{\gamma} + \mu_1^2 \mathcal{J} \tilde{\gamma}.$$

5.2 Calculations

To calculate the overlap and quadrupolar parts of the absorption coefficients, it is required to evaluate the radial distribution integrals \mathcal{I} and \mathcal{J} given by equations (17) and (18) respectively. For the high temperature region, the classical pair distribution function $g_0(x)$ in (17) and (18), which is equal to $\exp \{-v(x)/kT\}$ may be used. Here $v(x)$ is the Lennard-Jones intermolecular potential given by $v(x) = 4\epsilon(x^{-12}-x^{-6})$. For the intermediate temperature region, the classical expression for $g_0(x)$ is not valid and can be expanded as an asymptotic series in powers of Planck's constant. The resulting expressions of the integrals in equations (17) and (18) on consideration of the quantum effects can be expressed as,

$$(31) \quad \mathcal{I} = \mathcal{I}_{c1} - \Lambda^{*2} \mathcal{I}^{(2)} + \Lambda^{*4} \mathcal{I}^{(4)} + \dots$$

$$(32) \quad \mathcal{J} = \mathcal{J}_{c1} - \Lambda^{*2} \mathcal{J}^{(2)} + \Lambda^{*4} \mathcal{J}^{(4)} + \dots$$

where,

$$(33) \quad \Lambda^* = (h^2/2m_{00}\epsilon\sigma^2)^{1/2},$$

in which m_{00} is the reduced mass of the colliding pair of molecules of the type a-a or a-b. The numerical evaluation of the integrals \mathcal{I}_{c1} , $\mathcal{I}^{(2)}$, $\mathcal{I}^{(4)}$ and \mathcal{J}_{c1} , $\mathcal{J}^{(2)}$, $\mathcal{J}^{(4)}$ with the relation $\rho = 0.126\sigma$ have been done by Van Kranendonk and Kiss (1959) for reduced temperatures $T^* (= \frac{kT}{\epsilon}) = 1$ to 10.

As far as the integral \mathcal{J} is concerned, it does not involve ρ and hence may be taken as the same for all kinds of diatomic molecules

irrespective of any relation between ρ and σ . Thus, the quadrupolar part, $(\mu_1^2 + \mu_2^2) \mathcal{J} \tilde{\gamma}$, can be accurately calculated and consequently the relative line intensity distribution of the quadrupolar part of the binary absorption coefficients can be found. This has been done in this investigation by using the molecular parameters for deuterium given in Table XI. Here Q_1' , Q_2 , α_1' , α_2 of deuterium are assumed to be the same as those of hydrogen. By using equations (11) and (13) for pure deuterium gas and equations (27) and (29) for deuterium in deuterium-foreign gas mixtures, the binary absorption coefficients of the individual lines of the O and S branches, and the quadrupole part of the Q branch have been calculated. The results have been summarized in Table XIII. By fitting the experimental values of $\tilde{\alpha}_{1a}$ and $\tilde{\alpha}_{1b}$ with the theoretical expressions (23) and (30) respectively, the electron overlap and molecular quadrupole percentage contributions have been also calculated and presented in Table XII.

5.3 Variation of the Binary Absorption Coefficient with Temperature

To study the theoretical variation of the binary absorption coefficient of pure deuterium gas with temperature, it is necessary to evaluate both the radial integrals, \mathcal{I} and \mathcal{J} , given by (31) and (32) respectively. Van Kranendonk and Kiss (1959) have evaluated these integrals numerically using the relation $\rho = 0.126\sigma$. Though they assumed the relation $\rho = 0.126\sigma$ for hydrogen molecules, it is worthwhile to use the same relation for deuterium also. The overlap parameter λ^2 must then be determined empirically by fitting the theoretical expression (23) with

TABLE XI

Molecular Constants and parameters for deuterium and deuterium-foreign gas mixtures used in calculations.⁺

Mixture	ρ_{12}^i/k (°K)	σ_{12}^i (°A)	Λ_{12}^*	$\tilde{\gamma}_{12}^u$ (10 ⁻³² cm ⁶ sec ⁻¹)	$\frac{Q_1^g}{ea_0}$	$\frac{\alpha_1^p}{a_0^2}$	$\frac{\alpha_2}{a_0^3}$	$\frac{Q_2}{ea_0^2}$
D ₂ -D ₂	37.000	2.928	1.235	4.03	0.44	3.9	5.44 ^q	0.49 ^t
D ₂ -He	19.446	2.742	1.805	3.30	0.44	3.9	1.4 ^r	0
D ₂ -Ne	36.293	2.839	0.987	3.679	0.44	3.9	2.7 ^s	0

⁺ $\Lambda_{12}^* = (h^2/2m_{00} \epsilon \sigma^2)^{1/2}$ where m_{00} refers to the reduced mass of a(1) -b(2) pair of molecules; $a_0 = 0.529\text{\AA}$, Bohr's radius; e = electronic charge; and α_2 and Q_2 refer only to the perturbing molecules.

ⁱ Values for binary mixtures of gases are computed from those of the individual gases given by Hirschfelder, Curtis, and Bird (1954) using the relations ($\epsilon_{12} = (\epsilon_1 \epsilon_2)^{1/2}$ and $\sigma_{12} = \frac{1}{2}(\sigma_1 + \sigma_2)$).

^{g,p,q} See Hunt and Welsh (1964), Reddy and Cho (1965) and Pai (1965).

^r Stansbury, Crawford, and Welsh (1953).

^s Van Kranendonk (1958).

^t Poll and Van Kranendonk (1962)

^u $\tilde{\gamma}_{12} = (\pi e^2 \sigma_{12}^3)/3m_0 v_0$ where m_0 and v_0 are the reduced mass and the frequency of the molecular oscillation of deuterium.

TABLE XII

Electron overlap and molecular quadrupole parts of the binary absorption coefficients
of the induced fundamental band of D₂ and D₂-foreign gas mixtures

Temperature °K	Perturbing Gas	(Observed)	(Calculated)	(Observed)	Percentage	
		$\alpha_1 \times 10^{35}$ (cm ⁶ sec ⁻¹)	Quadrupole part $(\mu_1^2 + \mu_2^2) \bar{\nu} \times 10^{35}$ (cm ⁶ sec ⁻¹)	Overlap part $\lambda^2 \bar{\nu} \times 10^{35}$ (cm ⁶ sec ⁻¹)	Overlap (%)	Quadrupole (%)
273.16	D ₂ -D ₂	1.365	0.555	0.810	59.34	40.66
201.2	D ₂ -D ₂	1.225	0.525	0.700	57.14	42.86
77.3	D ₂ -D ₂	0.765	0.499	0.266	34.77	65.23
77.3	D ₂ -He	0.579	0.027	0.552	95.34	4.66
77.3	D ₂ -Ne	0.722	0.089	0.633	87.66	12.34

α_1 is α_{1a} for D₂-D₂ and α_{1b} for D₂-He and D₂-Ne.

TABLE XIII

The calculated line intensity distribution of the quadrupolar part of the binary absorption coefficients of the fundamental band of deuterium ($10^{-35}\text{cm}^6\text{sec}^{-1}$) at various temperatures in pure D_2 and D_2 -foreign gas mixtures

Temperature $^{\circ}\text{K}$	Perturbing Gas	0(4)	0(3)	0(2)	Q_{quad}	S(0)	S(1)	S(2)	S(3)	S(4)	Total (quadrupolar part)
273.16	$\text{D}_2\text{-D}_2$	0.012	0.015	0.043	0.143	0.110	0.073	0.111	0.028	0.020	0.555
201.2	$\text{D}_2\text{-D}_2$	0.005	0.010	0.039	0.128	0.139	0.082	0.100	0.018	0.004	0.525
77.3	$\text{D}_2\text{-D}_2$	-	-	0.011	0.076	0.297	0.089	0.025	0.001	-	0.499
77.3	$\text{D}_2\text{-He}$	-	-	0.001	0.004	0.016	0.004	0.002	-	-	0.027
77.3	$\text{D}_2\text{-Ne}$	-	-	0.002	0.015	0.053	0.014	0.005	-	-	0.089

the experimental value of $\tilde{\alpha}_{1a}$ at a certain temperature. As already described above, the quadrupole part, $(\mu_1^2 + \mu_2^2) \mathcal{J} \tilde{\gamma}$, has been calculated first using the molecular parameters for deuterium and is given in Table XII. By fitting the theoretical expression (23) with the observed value of $\tilde{\alpha}_{1a}$ at 0°C, λ^2 was found to be 4.225×10^{-5} (using the value of \mathcal{I} with $\rho = 0.126\sigma$).

From the present investigation and from the work of Chisholm (1952), Reddy and Cho (1965) and Watanabe and Welsh (1965) the experimental values of $\tilde{\alpha}_{1a}$ are known with sufficient accuracy between the temperatures 20°K and 300°K. An attempt has been made to calculate the theoretical values of $\tilde{\alpha}_{1a}$ for deuterium at various temperatures (by using the value of λ^2 obtained as mentioned above) with or without the consideration of quantum effects and to compare them with the available observed values. Thus a variation of $\tilde{\alpha}_1$ (or $\tilde{\alpha}_{1a}$) is shown in Fig. 18, and the values are listed in Table XV(b), which were obtained with $\rho = 0.126\sigma$ and $\lambda^2 = 4.225 \times 10^{-5}$ as mentioned above. It is seen that there is a fairly good agreement between the theoretical curve and the observed values of $\tilde{\alpha}_1$ at temperatures above 200°K, but the agreement seems to be poor below 200°K down to 20°K. Actually, to make a proper comparison in the low temperature region, one has to make use of ^{the} quantum mechanical pair distribution function for $g_0(x)$ to calculate the integrals \mathcal{I} and \mathcal{J} (instead of applying quantum corrections to the classical $g_0(x)$ as is done here). But this has not been done in this investigation.

A quantum mechanical treatment in the low temperature region has been used by Poll (1960) and the results for hydrogen have been summarized in the form of a "curve" by Watanabe and Welsh (1965).

For the case of hydrogen, the values of the binary absorption coefficients calculated by Poll (1960) by using ^{the} quantum mechanical pair distribution function are on the average 12% higher than the experimental values in the region 80°K to 20°K and 15% higher at 78°K. It is qualitatively estimated that the theoretical values of these coefficients obtained by Van Kranendonk by considering quantum corrections to the classical pair distribution function are about 25% higher than the experimental values at 78°K. This indicates that the quantum mechanical pair distribution function gives a better theoretical value than the quantum-corrected pair distribution function by an order of 13%. Assuming a similar situation for deuterium, it may be said that the quantum mechanical treatment would give a theoretical value for the absorption coefficient 15% higher than the experimental value at 78°K.

A qualitative study of the variation of the theoretical and observed values of α_1 of deuterium gas with temperature is made below by assuming various ratios of ρ and σ . The purpose is to find a suitable relation between ρ and σ , if there is any, which may possibly produce a better agreement between the theoretical and experimental values of α_1 throughout the temperature region, 300°K to 20°K. Since the radial integral \mathcal{J} is independent of ρ , the procedure is to make use of the integral values of \mathcal{J} given by Van Kranendonk and Kiss (1959) and to

calculate the various classical values of the integrals \mathcal{I}_{c1} corresponding to various ratios between ρ and σ . This has been done using the computer program for $\sigma/\rho = 2$ to 16 and the results obtained with $\sigma/\rho = 10.00$ and 11.80 and those with $\sigma/\rho = 7.94$ (i.e. $\rho = 0.126\sigma$) as obtained by Van Kranendonk and Kiss (1959) have been summarized in Table XIV. The theoretical values of $\tilde{\alpha}_1$ for different ratios of σ and ρ have been given in Table XV(a), XV(b) and XV(c).

No attempt has been done here either to consider the quantum corrections to the \mathcal{I}_{c1} values or to use a quantum mechanical pair distribution function for $g_0(x)$. For a complete and thorough quantitative investigation, these must be done. However, it is intended to limit the scope of the present work to qualitative estimation only. Based on what has been already discussed above, it is believed that this qualitative estimation would be good enough for our purpose to note some interesting features.

Figures 18 and 19 represent the semi-classical theoretical variations of $\tilde{\alpha}_1$ against temperature along with various observed points obtained by various authors including the present author. These curves were obtained by making use of quantum corrected integral values of \mathcal{J} (from Van Kranendonk and Kiss 1959) and by \mathcal{I}_{c1} values with σ/ρ equal to 10.00 and 11.80.

5.4 Conclusion

It is obvious from Figs. 18 and 19 that in all cases the theoretical value of $\tilde{\alpha}_1$ (for deuterium) decreases steadily as the temperature is lowered until a transition point is reached beyond which $\tilde{\alpha}_1$ increases rapidly with

TABLE XIV

Classical values of the radial (overlap) integral Π_{cl} for different ratios between ρ and σ

Reduced Temperature (T*)	$\rho = 0.0848\sigma$	$\rho = 0.100\sigma$	$\rho = 0.126\sigma$	
	Π_{cl}	Π_{cl}	$^+ \Pi_{cl}$	(For deuterium quantum corrected)
0.5	2.376	2.984	-	-
1.0	1.630	1.837	2.26	2.09
1.5	1.747	1.833	2.09	2.03
2.0	2.000	1.989	2.14	2.12
2.5	2.305	2.196	2.25	2.25
3.0	2.641	2.426	2.39	2.40
3.5	2.995	2.670	2.54	2.55
4.0	3.369	2.923	2.70	2.71
5.0	4.155	3.441	3.02	3.04
6.0	4.978	3.975	3.34	3.36
7.0	5.840	4.512	3.66	3.68
8.0	6.725	5.060	3.98	4.00
9.0	7.644	5.612	4.29	4.31
10.0	8.587	6.162	4.60	4.62

+Values obtained from Van Kranendonk and Kiss (1959)

TABLE XV(a)

Theoretical variation of binary absorption coefficient, $\tilde{\alpha}_1 (= \tilde{\alpha}_{1a})$ with temperature
for deuterium with $\rho = 0.100\sigma$ (i.e. $\sigma/\rho = 10.00$)

Temperature (°K)	Overlap part ($\lambda^2 \mathcal{H} \tilde{\gamma}$) ($10^{-35} \text{cm}^6 \text{sec}^{-1}$)	Quadrupolar part ($(\mu_1^2 + \mu_2^2) \mathcal{J} \tilde{\gamma}$) ($10^{-35} \text{cm}^6 \text{sec}^{-1}$)	$\tilde{\alpha}_1$ ($10^{-35} \text{cm}^6 \text{sec}^{-1}$)
40.0	0.3126	0.5907	0.903
50.0	0.3123	0.5477	0.860
60.0	0.3153	0.5142	0.830
70.0	0.3320	0.5030	0.835
77.4	0.3457	0.4991	0.845
80.0	0.3491	0.4980	0.847
90.0	0.3681	0.4955	0.864
100.0	0.3886	0.4948	0.883
120.0	0.4322	0.4974	0.930
150.0	0.5013	0.5064	1.008
180.0	0.5733	0.5171	1.090
201.2	0.6266	0.5253	1.152
240.0	0.7218	0.5409	1.263
*273.16	0.8105	0.5546	1.263
298.0	0.8670	0.5642	1.431

*Theoretical expression for $\tilde{\alpha}_1$ is fitted to the observed value of $\tilde{\alpha}_1$ at 0°C to obtain
 $\lambda^2 = 4.225 \times 10^{-5}$

TABLE XV(b)

Theoretical variation of binary absorption coefficient, $\tilde{\alpha}_1$, with temperature
for deuterium with $\rho = 0.126\sigma$ (i.e., $\sigma/\rho = 7.94$)

Temperature (°K)	Overlap part ($10^{-35}\text{cm}^6\text{sec}^{-1}$)	Quadrupolar part ($10^{-35}\text{cm}^6\text{sec}^{-1}$)	$\tilde{\alpha}_1$ ($10^{-35}\text{cm}^6\text{sec}^{-1}$)
40.0	0.4417	0.5907	1.032
50.0	0.4338	0.5477	0.982
60.0	0.4351	0.5142	0.949
70.0	0.4479	0.5030	0.951
77.4	0.4564	0.4991	0.956
80.0	0.4607	0.4980	0.959
100.0	0.4918	0.4948	0.987
120.0	0.5262	0.4974	1.024
150.0	0.5814	0.5064	1.088
180.0	0.6388	0.5171	1.156
201.2	0.6782	0.5253	1.204
240.0	0.7505	0.5409	1.291
*273.16	0.8105	0.5546	1.365
298.0	0.8567	0.5642	1.421

*The theoretical expression for $\tilde{\alpha}_1$ is fitted to the observed value of $\tilde{\alpha}_1$ at 0°C to obtain

$$\lambda^2 = 4.225 \times 10^{-5}.$$

TABLE XV(c)

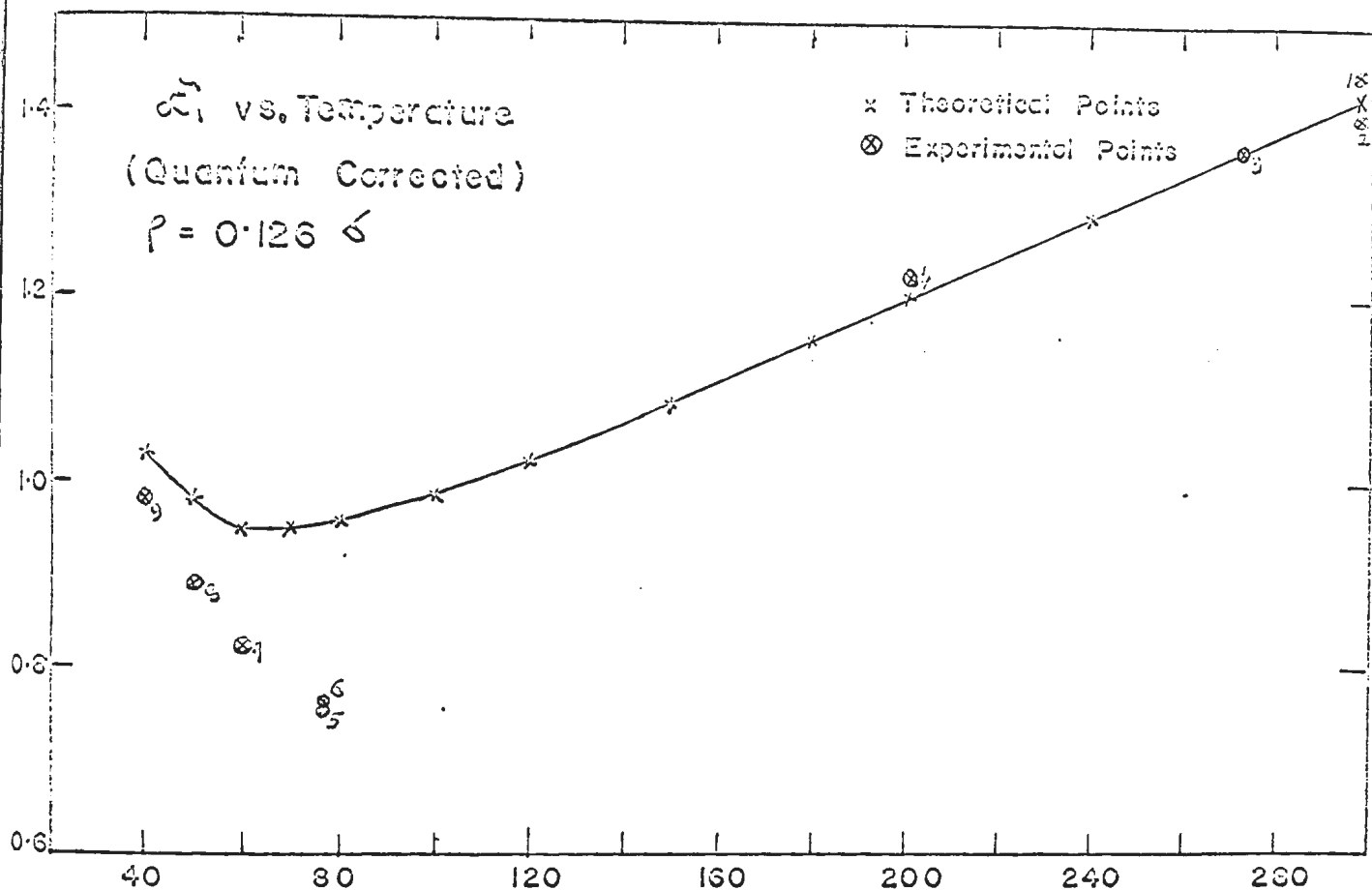
Theoretical variation of binary absorption coefficient, $\tilde{\alpha}_{1a}$ ($=\tilde{\alpha}_{1a}$) with temperature
for deuterium with $\rho = 0.0848\sigma$ (i.e., $\sigma/\rho = 11.80$)

Temperature (°K)	Overlap part ($\lambda^2 \mathbb{I} \tilde{\gamma}$) ($10^{-35} \text{cm}^6 \text{sec}^{-1}$)	Quadrupolar part [$(\mu_1^2 + \mu_2^2) \mathbb{J} \tilde{\gamma}$] ($10^{-35} \text{cm}^6 \text{sec}^{-1}$)	$\tilde{\alpha}_1$ ($10^{-35} \text{cm}^6 \text{sec}^{-1}$)
40.0	0.2151	0.5907	0.806
50.0	0.2216	0.5477	0.769
70.0	0.2518	0.5030	0.755
77.4	0.2701	0.4991	0.769
90.0	0.2966	0.4955	0.792
100.0	0.3199	0.4948	0.815
120.0	0.3685	0.4974	0.866
150.0	0.4471	0.5064	0.954
180.0	0.5306	0.5171	1.048
201.2	0.5914	0.5253	1.117
*273.16	0.8104	0.5546	1.365
298.0	0.8891	0.5642	1.453

*The theoretical expression for $\tilde{\alpha}_1$ is fitted to the observed value of $\tilde{\alpha}_1$ at 0°C to obtain

$$\lambda^2 = 4.225 \times 10^{-5}.$$

55



55

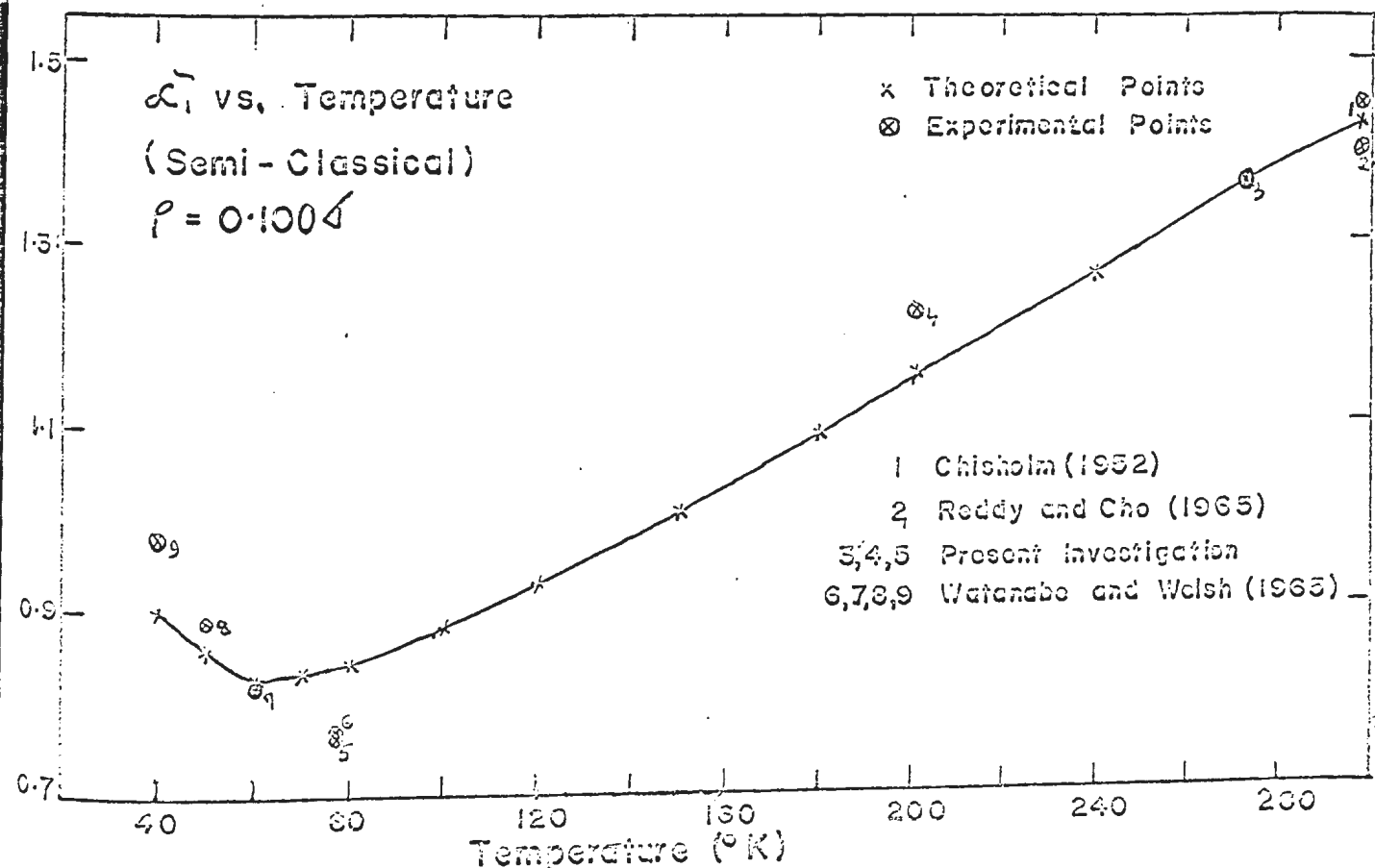


Fig. 19. Variation of α_1 With Temperature for Deuterium

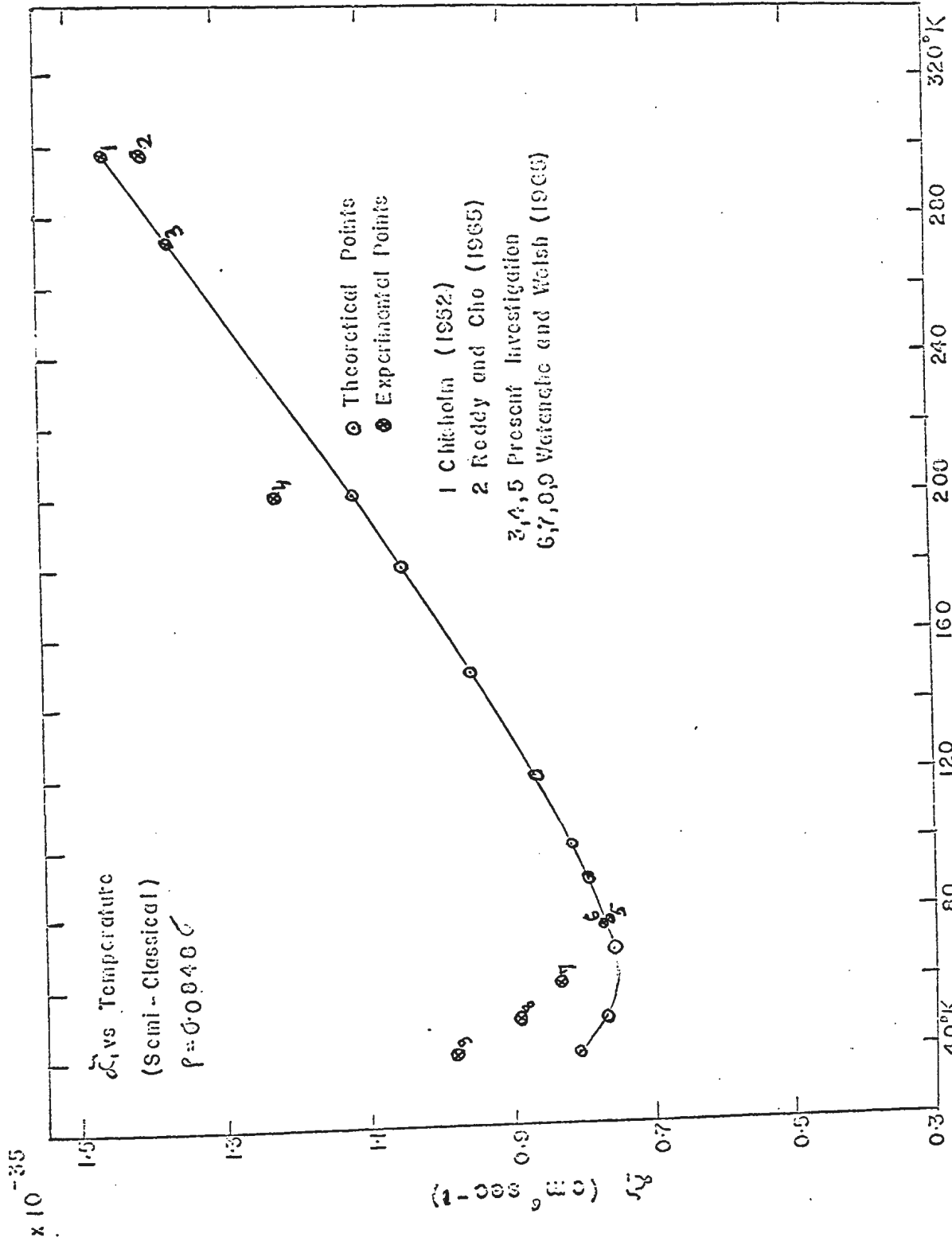


Fig. 19. Variation of \tilde{B}_2 With Temperature for Deuterium

the lowering of temperature. This trend in variation is analogous to the situation observed (experimentally) for deuterium (and also for hydrogen). In all cases, theoretically investigated here, it seems that $\tilde{\alpha}_1$ has a transition point around 60°K (for deuterium), while the observed transition point appears to be around 78°K (which can be established definitely only after bridging the gap between 80°K and 200°K from the experimental points). While a definite conclusion (for deuterium) must await the quantum mechanical treatment in the low temperature region on the lines adopted by Poll (1960), it is known from the report of Watanabe and Welsh (1965) that for hydrogen the quantum mechanical transition point of Poll (1960) is in accord with their experimental observation.

However, the fact that the observed rise in $\tilde{\alpha}_1$ for deuterium begins at a higher temperature than that for hydrogen, and is more rapid as the temperature is lowered, indicates simply a larger effect of bound states for deuterium, since the complex $(D_2)_2$ possessing three bound states will lie lower than the two bound states of the $(H_2)_2$ complex. This explanation is similar to that of Watanabe and Welsh (1965).

Figs. 18 and 19 further reveal that as one goes from a higher to a lower ratio of ρ/σ , the disagreement between the theoretical and experimental values of $\tilde{\alpha}_1$ becomes more pronounced at temperatures above 200°K, whereas there appears to be an apparent improvement in the situation around 80°K. This improvement is spurious due to a number of reasons. One should not forget that the quantum mechanical treatment in the lower

temperature region on the lines suggested by Poll (1960) would simply lower the theoretical values of $\tilde{\alpha}_1$ by an order of 10 to 15%, which would result in a larger discrepancy. The fact that the semi-classical value of $\tilde{\alpha}_1$ at 77°K for the ratio $\rho/\sigma = 0.0848$ (Fig. 19) and that it coincides better below 80°K for the ratio $\rho/\sigma = 0.100$ (Fig. 18), cannot be taken seriously because this type of coincidence can be obtained anyway at some temperature around 60°K by the choice of a suitable value for ρ/σ . But it must be said here that a quantum mechanical treatment alone can throw more light on the problem of variation of $\tilde{\alpha}_1$ with temperature in the low temperature region and this has not yet been done for deuterium.

Based on a simple reasoning, where one has to consider sufficient allowance for the most probable quantum correction up to 15%, it seems that a ratio around $\rho/\sigma = 0.126$ (probably, $\rho/\sigma = 0.130$) may give a relatively better agreement between the observed and the theoretical values of $\tilde{\alpha}_1$ for deuterium throughout the whole region, from 300°K to 20°K. But this obviously does not rule out the basic fact, that there remains on an average a discrepancy of 15 to 12% between the quantum mechanical and observed values of $\tilde{\alpha}_1$ for hydrogen in the low temperature region as given by Watanabe and Welsh (1965). Awaiting a quantitative estimation of the theoretical value of $\tilde{\alpha}_1$ based on the quantum mechanical treatment for the deuterium fundamental band, it may be assumed, for the time being, that the same order of discrepancy (15 - 12%) may exist between the quantum mechanical values and the observed values, of $\tilde{\alpha}_1$ for deuterium.

It seems that a single set of overlap parameters " λ " and " ρ/σ " is not able to give a proper agreement between the observed and the theoretical values of $\tilde{\alpha}_1$ in the region 300°K to 20°K. It looks apparent that the set of overlap parameters, λ and ρ , should be different at least for two temperature ranges - one below 80°K and the other above 80°K. This may reflect to some extent a temperature dependence of the overlap parameter λ or ρ .

Alternatively, it appears reasonable that for a fixed set of overlap parameters, λ and ρ , the theoretical expression for the absorption coefficient should include temperature dependent factors, which may produce a better agreement between the observed and calculated values of $\tilde{\alpha}_1$ than that existing at the present moment. The derivation of such factors must be based on an appropriate "model".

While no "modified exp-4" model involving the temperature dependence of λ or ρ has appeared as yet in the literature, a modified expression for the integrated absorption coefficient based on the statistical treatment of the absorption process has been reported recently by Sinha (1966).

Sinha (1966) has derived an expression for the collision-induced integrated absorption coefficient, which differs from the corresponding conventional expression (based on the Einstein coefficient of absorption) by a factor which is temperature dependent. This factor has been derived therein for three distinct temperature ranges.

REFERENCES

- (1) Allin, E. J., Gush, H. P., Hare, W. F. J., Hunt, J. L. and Welsh, H. L. 1959. Collog. intern., Centre Nat. (Paris), Rech. Sci. 77, 21.
- (2) Allin, E. J., Hare, W. F. J. et McDonald, R. E. 1955. Phys. Rev. 98, 554.
- (3) Briton, F. R. and Crawford, M. F. 1958. Can. J. Phys. 36, 741.
- (4) Chisholm, D. A. 1952. Ph.D. Thesis, University of Toronto, Toronto, Ont., Canada.
- (5) Chisholm, D. A. and Welsh, H. L. 1954. Can. J. Phys. 32, 291.
- (6) Cho, C. W., Allin, E. J. and Welsh, H. L. 1963, Can. J. Phys. 41, 1991.
- (7) Colpa, J. P. and Ketelaar, J. A. A. 1958. Mol. Physics.
- (8) DeGroot, S. R. and ten Seldam, C. A. 1947. Physica, 13, 47.
- (9) Dean, J. W. 1961. NBS Technical Note 120.
- (10) Ewing, G. E. and Trajman, S. 1964. J. Chem. Phys. 41, 814.
- (11) Gush, H. P., Hare, W. F. J., Allin, E. J. and Welsh, H. L. 1960. Can. J. Phys. 38, 176.
- (12) Hare, W. F. J. 1955, Ph.D. Thesis, University of Toronto, Toronto, Ont., Canada.
- (13) Hare, W. F. J., Allin, E. J., et Welsh, H. L. 1955. Phys. Rev. 99, 1887.
- (14) Hare, W. F. J. and Welsh, H. L. 1958. Can. J. Phys. 36, 88.
- (15) Herzberg, G. 1950. Spectra of Diatomic Molecules I.

- (16) Hirschfelder, J. L., Curtis, F. C. and Bird, R. B. 1954.
- (17) Hodgman, C. D. 1962. Handbook of Chem and Physics.
- (18) Hunt, J. L. and Welsh, H. L. 1964. Can J. Phys. 42, 873.
- (19) Ketelaar, J. A. A., Colpa, J. P. and Hooge, F. N. 1955. J. Chem. Phys. 23, 413.
- (20) Kiss, Z. J., Gush, H. P. and Welsh, H. L. 1959. Can. J. Phys. 37, 362.
- (21) Kiss, Z. J. and Welsh, H. L. 1959. Can. J. Phys. 37, 1249.
- (22) Mann, D. B. 1962, NBS Technical Note 154.
- (23) Michels, A., deBoer, J. and Bijl, A. 1937, Physica, 8, 347.
- (24) Michels, A. and Goudekot, M. 1941. Physica, 8, 347.
- (25) Michels, A., Wijker, H. and Wijkerh, 1949. Physics 15, 627.
- (26) Michels, A. and Wouters, H. 1941. Physica, 8, 923.
- (27) Michels, A., Wouters, H. and DeBoer, J. 1936, Physica 3, 585.
- (28) Michels, A., Graaff, W. , De Wassenaar, T., Levelt, J. M. H. and Louwerse, P. 1959. Physica, 25¹, 28.
- (28)₁ Pai, S. T. 1965, Thesis, Memorial University of Newfoundland.
- (29) Pai, S. T., Reddy, S. P. and Cho, C. W. 1966. Can. J. Phys. 44, 2893.
- (30) Poll, J. D. and Van Kranendonk, J. 1962. Can. J. Phys. 40, 163.
- (31) Poll, J. D. 1960. Ph.D. Thesis, University of Toronto, Toronto, Ontario, Canada.
- (32) Racah, G. 1942. Phys. Rev. 61, 186, 1942, Phys. Rev. 62, 438, 1943, Phys. Rev. 63, 968.
- (33) Reddy, S. P. and Cho, C. W. 1965a. Can. J. Phys. 43, 793, and 1965b, Can. J. Phys. 43, 2331.
- (34) Sinha, B. B. P. 1966. Physica, 32, 1033-47.
- (35) Stoicheff, B. P. 1957. Can. J. Phys. 35, 730.

- (36) Thomson, H. W. 1961. I.U.P.A.C.
- (37) Timmerhaus, K. D. 1963. Advances in Cryogenic Engineering, Plenum Press, New York. Vol. 8, 135-45.
- (38) Van Kranendonk, J. and Bird, R. B. 1951. Physica, 17, 953 and 968.
- (39) Van Kranendonk, J. 1952. Ph.D. Thesis on the Theory of Pressure Broadening and Pressure Induced Absorption, University of Amsterdam, Amsterdam, Netherlands.
- (40) Van Kranendonk, J. 1957. Physica, 23, 825.
- (41) Van Kranendonk, J. 1958. Physica, 24, 347.
- (42) Van Kranendonk, J. and Kiss, Z. J. 1959. Can. J. Phys. 37, 1187.
- (43) Watanabe, A. and Welsh, H. L. 1964. Phys. Rev. Letters, 13, 810.
- (44) Watanabe, A. and Welsh, H. L. 1965. Can. J. Phys. 43, 818.
- (45) Woolley, H. W., Scott, R. B., and Brickwedde, F. G. 1948. Journal of Research, NBSRP (1932), 41, 396-434.
- (46) Welsh, H. L, Crawford, M. F. and Locke, J. L. 1949, Phys. Rev. 76, 580.
- (47) Welsh, H. L, Crawford, M. F., McDonald, R. E. and Chisholm, D. A. 1951, Phys. Rev. 83, 1264.

ACKNOWLEDGEMENTS

The work presented in this thesis was supervised by Professor C. W. Cho to whom the author is greatly indebted and obliged for guidance and assistance in all aspects leading to the present thesis.

The author is also indebted and obliged to Professor S. P. Reddy for his frequent discussions and assistance during the experimental work and preparation of the thesis, and to Professor S. W. Breckon for his encouragement and discussion during the period of research.

The financial assistance in the form of a teaching fellowship, awarded during 1964-66, was gratefully received from Memorial University of Newfoundland.

The author gratefully acknowledges the cooperation and assistance of the Staff of Technical Services of Memorial University, headed by Mr. W. Gordon, in the design and construction of a low temperature and high pressure cell and in other technical problems.

The use of the computer facilities in the Mathematics Department of Memorial University of Newfoundland is gratefully acknowledged.

Thanks are also due to Mr. A. Walsh and Mr. S. Tak for their assistance in preparing some of the diagrams in this thesis.

The author also wishes to thank Mr. S. T. Pai for the use of several diagrams from his M.Sc. Thesis.

